Journal of Food Composition and Analysis 107 (2022) 104288

Contents lists available at ScienceDirect

Journal of Food Composition and Analysis

journal homepage: www.elsevier.com/locate/jfca

Original Research Article

Non-destructive determination of color, titratable acidity, and dry matter in intact tomatoes using a portable Vis-NIR spectrometer

Annelisa Arruda de Brito [a,*], Fernanda Campos [b], Abadia dos Reis Nascimento [c], Clarissa Damiani [d], Flávio Alves da Silva [d], Gustavo Henrique de Almeida Teixeira [e], Luis Carlos Cunha Júnior [c]

[a] Universidade Federal de Goiás, Escola de Agronomia, Programa de Pós-Graduação em Agronomia, Universidade Federal de Goiás Rodovia Goiânia-Nova Veneza, Km 0 s/n Campus - Samambaia, Goiânia, GO, 74690-900, Brazil
[b] Universidade Federal de Goiás, Escola de Agronomia, Universidade Federal de Goiás Rodovia Goiânia-Nova Veneza, Km 0 s/n Campus - Samambaia, Goiânia, GO, 74690-900, Brazil
[c] Universidade Federal de Goiás, Escola de Agronomia, Departamento de Horticultura, Universidade Federal de Goiás Rodovia Goiânia-Nova Veneza, Km 0 s/n Campus - Samambaia, Goiânia, GO, 74690-900, Brazil
[d] Universidade Federal de Goiás, Escola de Agronomia, Departamento de Engenharia de Alimentos, Universidade Federal de Goiás Rodovia Goiânia-Nova Veneza, Km 0 s/n Campus - Samambaia, Goiânia, GO, 74690-900, Brazil
[e] Universidade Estadual Paulista (UNESP), Faculdade de Ciências Agrárias e Veterinárias (FCAV), Campus de Jaboticabal, Via de Acesso Prof. Paulo Donato Castellane s/n. Jaboticabal, São Paulo, CEP: 14.884-900, Brazil

ARTICLE INFO

Keywords:
Chemometrics
Principal component analysis
Partial least square
Portable Vis-Nir
Quality food

ABSTRACT

Fruit color and chemical composition, particularly dry matter and titratable acidity (TA), are important tomato-quality parameters for consumers. Therefore, a single test allowing for the evaluation of these parameters simultaneously would improve the efficiency of this analysis. Vis-NIR spectroscopy has been used to identify many compounds in fruits and vegetables, therefore, here, a portable Vis-NIR spectrometer was used to collect the spectra of fresh tomatoes produced from November 2018 to November 2019, in five tomato cropping regions in Brazil, namely, Goiás, Bahia, Santa Catarina, Minas Gerais, and São Paulo states. Calibration and prediction models were developed using the 396–1,131 nm spectral region, through principal component analysis (PCA), and partial least square regression (PLS). Strong prediction results (root mean square of error prediction, RMSEP; coefficient of prediction, Rp^2; and standard deviation ratio, SDR) were obtained for the color parameter a^*, representing red (RMSEP = 2.89, Rp^2 = 0.94, SDR = 4.11), and the amount of dry matter (RMSEP = 0.46 %; Rp^2 = 0.59 % SDR = 1.92). However, poor prediction results were obtained for titratable acidity (RMSEP = 0.07 %; SDR = 1.15). These findings indicate that color (a*) and dry matter of intact tomatoes may be predicted using a portable Vis-NIR spectrometer.

1. Introduction

Currently, there is an increasing demand for high-quality agricultural products, which requires inspection processes of the supply chains of producers and distributors to guarantee superior-quality products to consumers (Cortés et al., 2019). The evaluation of external and internal attributes related to fruit postharvest quality is generally conducted destructively, which is time consuming, and may require large amounts of chemical reagents and the use of many samples (Porep et al., 2015); furthermore, it can be quite wasteful in terms of the number of samples required.

Among destructive tomato-quality analyses, Moretti (2006) showed a protocol summarizing the methodologies used in postharvest tomato-quality evaluation. Within the procedures mentioned are, the determination of total soluble sugars, total vitamin C content, total carotenoids content, total titratable acidity, total soluble solids, leakage of solutes from pericarpic tissue, total chlorophyll, and chlorophyll *a* and *b* contents, evolution of carbon dioxide and ethylene, firmness, and color

* Corresponding author.
E-mail addresses: annelisabrito@gmail.com (A. Arruda de Brito), fecolag@gmail.com (F. Campos), abadiadosreis@ufg.br (A. dos Reis Nascimento), clarissadamiani@ufg.br (C. Damiani), flaviocamp@ufg.br (F. Alves da Silva), gustavo.teixeira@unesp.br (G.H. de Almeida Teixeira), cunhajunior.l.c@ufg.br (L.C. Cunha Júnior).

https://doi.org/10.1016/j.jfca.2021.104288
Received 16 July 2021; Received in revised form 10 October 2021; Accepted 16 November 2021
Available online 18 November 2021

(L*a*b*) (Dubois et al., 1956; Terada et al., 1979; Lime et al., 1957; Moretti et al., 1998; Whitlow et al., 1992; Inskeep and Bloom, 1985; Moretti, 2006).

However, alternative non-destructive technologies are available for evaluating these attributes, including, X-ray transmission, acoustic transmission, resonance frequency, and near infrared spectroscopy (NIRS). Among these, the latter shows the highest commercial adoption rates (Walsh et al., 2020), because of the ease for its application, and low cost, compared to the other technologies mentioned. Furthermore, the use of Vis-NIR spectroscopy is increasingly common because it is a convenient, non-destructive, and fast analytical method that requires minimal sample preparation, and is applicable to complex samples (Menezes et al., 2014).

Near-infrared spectroscopy allows for the continuous monitoring of compounds that may be related to the nutritional value and flavor of the analyzed products (Beghi et al., 2017) and has been commonly applied to quantify and predict postharvest fruit and vegetable internal-quality attributes (Amodio et al., 2017; Escribano et al., 2017). Infrared spectroscopy is based on the absorbance of radiation at molecular vibrational frequencies occurring in the O—H, N—H, and C—C, C—O, C—N, and N—O groups in organic materials. The overtone and combination vibrations of the first group dominate the NIR region (700–2500 nm), while those of the second group absorb in the mid-infrared region (MIR) (2500–25,000 nm); and electronic transitions absorb in the visible region (400–700 nm) and the ultraviolet (250–400 nm) region (Cortés et al., 2019; Beghi et al., 2017).

The combination of these absorption bands and overtones corresponds to the vibration frequencies between the atomic bonds of the analyzed material, and each component has a unique combination of atoms; therefore, no compound will produce the same Vis-NIR spectra. However, the applicability of the technique requires the support of chemometric models, which in turn is time consuming and requires expertise and experience from researchers and technicians. NIRS can be applied to study biochemical alterations in fruit and vegetables during ripening, which is a homogeneous process for the entire fruit, both in the pulp and the epidermis, each of which can be represented by one spectral pattern (Beghi et al., 2017).

Based on the relationship between the chemical alterations and the resulting spectral patterns, it is possible to analyze the various quality attributes of intact tomatoes. Among several factors evaluated through NIRS, studies have reported the use of this technology, primarily for determining soluble solid content (SSC) and titratable acidity (TA), as well as color (L*a*b*, Chroma and hue angle), maturity stage, pH, gustative index, and firmness (Camps et al., 2012; Sirisomboon et al., 2012; Ecarnot et al., 2013; Saad et al., 2014; Torres et al., 2015; Saad et al., 2016; Acharya et al., 2017; Beghi et al., 2018; Feng et al., 2019; Castrignanò et al., 2019; Ibáñez et al., 2019; Ramos-Infante et al., 2019; Brito et al., 2021).

These studies evaluated the use of near-infrared spectroscopy not only with bench spectrometers but also with portable spectrometers for the detection of quality attributes in intact tomatoes. Herein, we demonstrate the viability of using a commercial, portable Vis-NIR spectrometer (F-750) to evaluate tomato fruit-quality parameters in larger fruit batches than allowed by traditional methods. Given the importance of quality attribute determination, the use of a single device that allows for the evaluation of these parameters simultaneously will improve the analytical efficiency. Therefore, this study aimed to analyze and model external (color) and internal (titratable acidity and dry matter) intact tomato-quality attributes, using a portable Vis-NIR spectrometer.

2. Material and methods

2.1. Plant material

Tomato fruits (*Solanum lycopersicum* L.) of the Salad variety were obtained weekly from November 2018 to November 2019 at the Centrais de Abastecimento de Goiás (CEASA-GO), Goiânia, Brazil. During this period, fruits available for commercialization were collected and identified according to their origin and year of collection, that is, Goiás, Paraná, São Paulo, Bahia, Minas Gerais, or Santa Catarina state, and 2018 or 2019 (Table 1). Tomato maturity stages were defined as pinkish, red, and red ripeness, where pinkish is characterized as 30%–60% of the fruit being red, red is defined as having between 60 % and 90 % of red on the surface, and red ripeness is defined as more than 90 % of the fruit surface being red (Batu, 2004).

2.2. Vis-NIR spectral data acquisition

After temperature stabilization (~20 °C), Vis-NIR spectra were collected from one spectrum at three distinct points (Fig. 1), one for each reference analysis: the first point for color, the second for the titratable acidity (TA), and the third for dry matter (DM). Because the fruit is not internally homogeneous, the spectra were collected in the fruit epidermis precisely in the equatorial region (Guthrie et al., 2005), which corresponds to the center line of the fruit. This region has been used for tomato NIR analysis in previous studies aiming to evaluate quality parameters (Camps et al., 2012; Acharya et al., 2017; Huang et al., 2018; Radzevičius et al., 2016; Alenazi et al., 2020).

A portable Vis-NIR spectrometer (Felix Instruments, model F-750, Camas, WA, USA) was used with a tungsten xenon lamp as the light source. Vis-NIR spectra were collected in interactance mode at wavelengths ranging from 280 to 1200 nm, with a resolution of approximately 3 nm and an optical resolution of 8–13 nm (depending on wavelength).

2.3. Reference analysis

Following the acquisition of the Vis-NIR spectra, reference analyses were performed. For this, data related to fruit color were collected using a colorimeter (Minolta, model CR-400, Osaka, Japan). Color was expressed as L*, a*, and b* according to *the Commission Internationale de l'Éclairage* (CIE), and chromaticity (Chroma) and hue angle *(°h)* were calculated after McGuire (1992).

Second, titratable acidity (TA) was measured. Cylinders with an approximate diameter of 30 mm and a depth of 20 mm were removed, macerated in a porcelain mortar, and the pulp obtained was weighed, tabulated, diluted in 20 ml of distilled water, and titratable acidity (TA) was calculated using Eq. (1). Bromothymol blue (1 %) was added to the solution, which was then titrated with a 0.01 N NaOH solution. The results were expressed in citric acid equivalents per 100 g, according to AOAC method no. 942.15 (AOAC, 1997).

$$TA_{(g/100g)} = \frac{n \times N \times Eq}{p}, \quad (1)$$

where:

n = NaOH solution volume (ml) used in the titration;
N = normality of NaOH solution;
Eq = citric acid equivalent; and
p = sample weight (g).

Finally, at the third point, to evaluate dry matter (DM) content, cylinders approximately 30 mm in diameter and 20 mm in depth, were removed and transferred to a forced air-circulation oven (SolidSteel, SSD, Brazil) at 105 °C until constant weight (Radzevičius et al., 2016).

2.4. Quimiometrics analysis

To develop the calibration and prediction models, both the Vis-NIR spectra and reference values were separated according to the place of origin and year of collection (2018 and 2019). Only the TA analysis was evaluated in both years of collection, while color and DM evaluations

Table 1
Systematic Bibliographic Review of works using near infrared spectroscopy (NIRS) to evaluate quality parameters in tomatoes fruit in the last 10 years (2010 – 2012).

Quality parameter	Equipment	n	R^2c	RMSEC	R^2p	RMSEP or SEP	SDR	Year	Reference
Firmness, Soluble Solids Content and Titrable Acidity	Spectrometer (USB4000, Ocean Optics Inc., U.S. A.) 471.4~1153.7 nm	180	Firmness: 0,934; SSC: 0,949; AT: 0,782		Firmness: 0,859; SSC: 0,869; AT: 0,596	SEP Firmness: 1,8994; SSC: 0,3423; AT: 0,2095		2010	[Kim et al., 2010]
Size estimation	VIS-NIR mobile spectrometer fiber type (agrospec, Tec5 Co., Germany) 350-2200 nm	618 (cal) 202 (val)	0,77 - 0,80	4,43 - 5,55	0,69 - 0,74	RMSEP 4,87 - 6,46	1,80 - 2,35	2011	[Yang et al., 2011]
Growing stage and harvest time	VIS-NIR mobile spectrometer fiber type (agrospec, Tec5 Co., Germany) 350-2200 nm plus two ingaas senors (1000 - 2200nm)	60	0,93 0,87 & 0,91 (cv. 1 2 & 3)	0,084 0,111 & 0,088 (cv 1, 2 & 3)	0.91 0,92 e 0.92 9 (cv 1, 2 & 3)	RMSEP 0.097 0,084 & 0,080 (cv 1,2 & 3)	3.29 3.70 & 3,49 (cv 1, 2 & 3)	2011	[Yang et al., 2011]
Soluble solids, dry matter, acidity, glucose, fructose, citric and malic acids contents	Bruker Tensor 27 FTIR spectrometer (Wissembourg, France) equipped with a horizontal attenuated total reflectance (ATR) sampling accessory and deuterated triglycine sulphate (DTGS) detector	450 (cal: 260; val ('07: 80; val '08: 110)	Dry matter 0,97; SS 0,99; Glucose 0,97; Fructose 0,91; Total acidity 0,96; citric acid 0,95; malic acid 0,91	DM: 0,198; SS: 0,128; glucose: 0,063; Fructose: 0,095; TA: 0,354; Citric acid: 0,029; malic acid: 0,017	DM: 0,96; SS: 0,98; glucoe: 0,96; fructose: 0,92; TA: 0,96; citric acid: 0,94; malic acid: 0,88	RMSPE DM: 0,256; SS: 0,162; glucose: 0,081; fructose: 0,102; TA: 0,363; citric acid: 0,034; malic acid: 0,019		2011	[Ścibisz et al., 2011]
Optimal harvest time in cherry tomatoes	Mobile, fibre-type, VIS-NIR spectrophotometer (agrospec, Tec 5, Germany) with spectral range of 350-2200 nm,	217 cal 57 val	0,89	2,51	0,9	RMSEP 2,5	3,01	2011	[Yang et al., 2011]
Maturity and textural properties, soluble solids, insoluble solids	BRAN + LUEBBE infraalyzer 500 (Bran + Luebbe Gmbh, Germany), 1100–2500 nm	72	SSC = 0,77; Insoluble solids = 0,77; Compression test = 0,05 - 0,98; puncture test = 0,5 - 0,99		SSC = 0,80; insoluble solids = 0,56; Compression test = 0,21 - 0,86; puncture test = 0,28 - 0,95	SEP SSC = 0.210; IS = 0.0026; compression test =1.43x10-5 ~ 5,19; puncture test = -0,12 ~0,67	SSC = 1,62; Insoluble solids = 1,00; Compression test = 1,00 - 2,00; puncture test = 0,90 - 2,17	2012	[Sirisomboon et al., 2012]
Firmness, soluble solids and color (cv. Climberley)	Spectrometer NIR portable (PHASIR 0917, Analyticon Instruments, Germany) 690-1700nm	38		SSC =0,35; firmness =5,1; L* = 1,96; a* = 2,91	SSC =0,69; firmness =0,88; L* = 0,95; a* = 0,92	RMSEP SSC =0,40; firmness =5,9; L* = 2,26; a* = 3,02		2012	[Camps & Gilli, 2012]
Lycopene	Corona fibre visnir (1104-400, zeiss, germany)	32	0,9 mg/100g		0.92 mg/100g	SEP 0.65 mg/100g		2012	[Berra, 2012]

were only performed in 2019. To avoid any bias, the calibration and prediction sets were separated using the Kennard-Stone algorithm (Kennard and Stone, 1969) owing to its adaptation to analytical chemistry applications and its ability to allow a training model to cover most sources of variation within the dataset, thus, ensuring that the training model is more representative of the whole dataset (Morais et al., 2019). Therefore, the following populations were constructed according to the analyzed parameters:

Color: The models were developed using 2019 data, 2/3 of the data were used for the calibration population and 1/3 for the prediction population, aiming to represent the factors that affect the NIR spectrum and those related to seasonal variations (Pasquini, 2003), and were selected to represent the whole range of variability (Conzen, 2003); therefore, the two populations contained fruit from the state of Goiás (GO, n = 1559), Paraná (PR, n = 12), São Paulo (SP, n = 12), Minas Gerais (MG, n = 243), and Santa Catarina (SC, n = 24) (Table 2).

Titratable acidity (TA): For the models related to the TA data, the calibration and prediction populations were divided into population 1 (Pop1) with data from 2018 and fruits from the states of Goiás (GO, n = 209), Paraná (PR, n = 20), São Paulo (SP, n = 20), and Bahia (BA, n = 10); and population 2 (Pop2) with data from 2019 with fruits from the states of Goiás (GO, n = 1,551), São Paulo (SP, n = 32), Minas Gerais (MG, n = 197), and Santa Catarina (SC, n = 16) (Table 3).

Dry matter (DM): The models for DM content were developed using data from 2019 and contained information from the states of Goiás (GO, n = 1,294), Paraná (PR, n = 11), São Paulo (SP, n = 25), Minas Gerais (MG, n = 228), and Santa Catarina (SC, n = 24) (Table 4).

2.4.1. Model development

For model development, the Vis-NIR spectra were used without pre-processing and after pre-processing. Standard normal variation (SNV) was applied to reduce the effects of uncontrolled baseline and intensity variations in the spectra (Camps et al., 2012), and Multiplicative Scatter Correction (MSC) pre-processing was applied to correct the data (Windig et al., 2008). Additionally, Orthogonal Scatter Correction (OSC) was used to minimize variability unrelated to the analyzed variable (Blanco et al., 2001). By applying these pre-processing procedures, complications such as scattering and base lights could be corrected (Saad et al.,

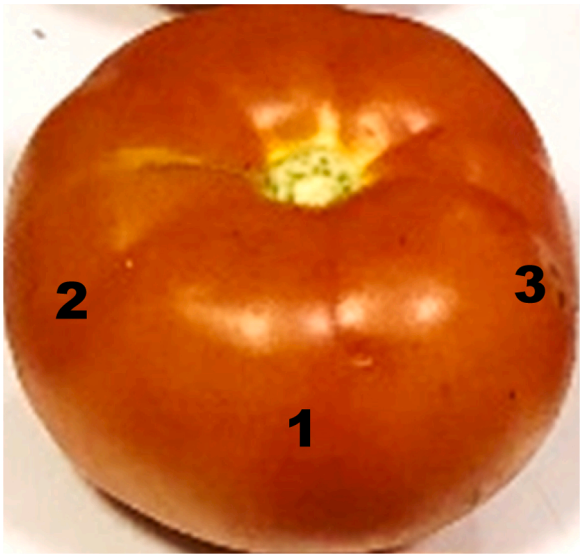

Fig. 1. Representation of the points where the spectra were obtained for each reference value, in which: 1 – color parameters L*a*b*C*h° reference values; 2 – titratable acidity reference values; and 3 0 dry matter reference values.

2014). In addition, the first and second Savitzky Golay derivatives (Savitzky and Golay, 1964) were used with second-order polynomials with smooth windows of 7 (3 + 3), 9 (4 + 4), 13 (6 + 6), 15 (7 + 7), 21 (10 + 10), 23 (11 + 11), and 25 (12 + 12) points for the first and second derivatives, respectively. Unscrambler software (10.4, CAMO, Oslo, Norway) was used for the analysis.

Principal Component Analysis (PCA) was conducted with full cross validation to determine the best factor number for the Partial Least Square Regression (PLSR). The wavelength ranges used were 501–702 nm in the visible region, 702–1104 nm in the near-infrared region, 729–975 nm (Acharya et al., 2017) and 396–11,131 nm with full spectra. PLSR was performed to develop linear prediction models between the spectra and reference values of each analyzed parameter, and full cross-validation was performed in the developed models.

2.4.2. Model selection

The performance of the models was assessed by the coefficient of determination of the calibration set (R^2c), cross-validation (R^2cv), the root mean square error of calibration (RMSEC), root mean square error of cross-validation (RMSECV), and the ratio between the standard deviation (SD) of the calibration population and the RMSEC (SDRcv).

The following parameters were considered for the prediction: coefficient of determination (R^2p), bias, root square of the mean quadratic error of prediction (RMSEP), and the ratio between the SD of the prediction population and the bias-corrected RMSEP (SDRp). The relationships among RMSEP, bias, and SEP were evaluated using the following equation: $RMSEP^2 = SEP^2 + bias^2$ (Golic and Walsh, 2006). The use of SDR statistics allowed for the comparison of model performance across the population with different SDs, as shown by the equation for calibration: SDRcv = SD/RMSECV, where SD is the standard deviation of the calibration, and the equation for prediction is SDRp = SDp/RMSEP, where SDp is the standard deviation of the prediction set (Golic and Walsh, 2006). To be considered applicable, the models must have high coefficients of correlation (He et al., 2005), low RMSEC and RMSEP (Magwaza et al., 2012), SDR values higher than 1.5 (Nicolai et al., 2007), and a relatively low number of latent variables, which is generally desirable to eliminate noise in the model (He et al., 2005).

3. Results and discussion

3.1. Vis-NIR spectra

The Vis-NIR spectra of the sampled tomatoes are shown in Fig. 2. In the visible region, a peak was observed in the yellow area (507 nm), which might be associated with the presence of carotenoid compounds. Similarly, a peak observed in the red region (675 nm) might also be related to the presence of carotenoids, specifically lycopene, which is abundant in tomatoes (Gómez et al., 2006). The absence of a peak in the green region (500–565 nm) indicates that the fruit was ripe because chlorophyll is present only in immature fruits (Subedi and Walsh, 2020).

In the near infrared region (NIR), a peak was observed between 915 nm and 1,030 nm (Fig. 2). According to Feng et al. (2019), this peak is the result of the presence of water in the fruit, as absorption bands of the O—H group can be observed at 740, 840, 960, and 1,440 nm (Subedi and Walsh, 2020). Therefore, the Vis-NIR spectra are characteristic of fully ripened tomatoes, as a result of the higher absorbance in the yellow and red regions, as well as the presence of a large quantity of water due to the high absorbance in the 970 nm region.

For the development of the models, we used both the Vis-NIR spectra with (Fig. 2) and without (Fig. 3A) SNV pre-processing and MSC (Fig. 3B) to correct the Vis-NIR spectra and align them with reference spectra (Windig et al., 2008) after the OSC pre-processing (Fig. 3C) to minimize the alterations that were not related to the analyzed variables (Blanco et al., 2001). The Savitzky-Golay first derivative (Fig. 4A) and second derivative (Fig. 4B) were then applied.

3.2. Reference analysis

There was a significant difference ($p < 0.05$) in color parameters (Table 5), in TA, and in DM (Table 6) for tomatoes from different origins. Tomatoes from the state of Goiás showed the highest mean for the color parameters L*, b*, C*, and h°, with fruits from Paraná having the highest mean for the color parameter a* (Table 5); meanwhile, tomatoes from the state of Bahia showed the highest mean TA values, and fruit from Santa Catarina showed the highest mean DM values (Table 6).

Thus, tomatoes from the state of Goiás can be classified between turning and pink maturity stages, whereby the tomatoes in the turning stage have a yellowish, pink, or red color on 10 %–30 % of their surface, while, in the pink stage, they show a pink or red color between 30 % and 60 % of the fruit surface. In contrast, tomatoes from the state of Paraná returned higher means for color parameter a*, referring to red, and can be classified as tomatoes in the light red stage, when more than 60 % of the surface shows a pinkish-red or red color, or the red ripe stage, meaning that the fruit surface is more than 90 % red (Ferreira et al., 2004).

Overall, tomatoes from the state of Paraná showed a reddish color (López and Gómez, 2004), with the fruits from this state showing the highest mean a* values. Chroma (C*) was the only color parameter for which no difference was detected among tomatoes from different states.

The TA values for tomatoes from the states of Goiás, São Paulo, Minas Gerais, Santa Catarina, and Paraná did not differ statistically. However, fruit from Bahia showed statistically significant differences in TA values in relation to the other states, except for the state of São Paulo. Further, we observed low TA values (0.21 %–0.30 %, Table 6), in relation to the values reported by Saad et al. (2014), which were 0.48 %–0.59 %.

Table 2
Systematic Bibliographic Review of works using near infrared spectroscopy (NIRS) to evaluate quality parameters in tomatoes fruit in the last 10 years (2013 – 2015).

Quality parameter	Equipment	n	R^2c	RMSEC	R^2p	RMSEP or SEP	SDR	Year	Reference
Hue, Chroma, SSC, ph, firmness and water content	Field Spectrometer (LabSpec 5000, Analytical Spectral Devices, Inc.)	Hue (367), Chroma (367), SSC (319), pH (142), firmness (332) and water content (198)	Hue (0,99), Chroma (0,91), SSC (0,87), pH (094), firmness (0,82), water content (0,84)				Hue (10,7), Chroma (3,24), SSC (2,42), pH (3,45), firmness (2,14), water content (2,08)	2013	[Ecarnot et al., 2013]
Maturity	Portable spectrometer (Model Nirvana-Analytical Spectrometer, Integrated Spectronics, Sydney, Australia)	350	Variety specific models correctly identified 75–85% of immature tomatoes and 82–86% of mature green tomatoes in internal cross-validation	False positive rates varied from 3% to 40% and 0% to 31% respectively	A 'global' model, correctly predicted 71% of immature and 85% of mature green tomatoes, with false positive error rates of 13% and 22%, respectively, in internal cross-validation of both varieties			2013	[Tiwari et al., 2013]
Firmness. Sugar content °brix, TA % in cherry tomatoes	VIS/NIRS (USB4000, Ocean Optics Inc., USA),	180	firmness: 0,87; sugar content: 0,86; TA: 0,7	firmness: 1,86; sugar content: 0,33; TA: 0,18	firmness: 0,88; sugar content: 0,86; TA: 0,54	RMSEP firmness: 1,70; sugar content: 0,34; TA: 0,22		2013	[Kim et al., 2013]
Soluble solids content (SSC) and TA	Reflectance mode (log1R/1) using a multi-purpose analyser (MPA) spectrometer (Bruker Optics)	150		0,13; 0,55	SSC: 0,52 TA: 0,51	RMSEP 0,53;0,73		2014	[Oliveira et al., 2014]
SSC, ph, titratable acidity and lycopene	VIS/NIR spectroscopy (Avantes BV, Netherlands) 299-1100 nm	143	SSC = 0,99; lycopene = 0,99; TA =0,98; pH =0,98	SSC = 0,02; lycopene = 0,88; TA = 0,88; pH = 0,025	SSC = 0,99;lycopene = 0,99; TA =0,98; pH =0,98	RMSEP SSC = 0,02; lycopene = 0,91; TA =0,90; pH =0,0,37		2014	[Saad et al., 2014]
SSC, lycopene and polyphenols	Spectrometer FieldSpec HandHeld 2™ (Analytical Spectral Devices Inc., Co. USA)	61	SSC =0,88; lycopene = 0,91; polyphenols=0,81	SSC =0,39; lycopene = 1,27; polyphenols =6,53	SSC =0,77; lycopene= 0,75; polyphenols =0,72	RMSEP SSC =0,51; lycopene = 1,99; polyphenols =7,63		2014	[Szuvandzsiev et al., 2014]
Effects of simulated transport vibration on tomato tissue damage	Spectrometer Qualityspec Pro (ASD Inc., Boulder, CO, USA)	230 (cal) 50 (val)	0,985	0,116	0.984	RMSEP 0.137		2014	[Wu & Wang, 2014]
Ripeness classification (PLS-DA)	Optical Property Analyzer' (OPA)	280 'Sun Bright' tomatos at different ripeness grades	92.1%, 84.4%, 92.3%, and 92.1% classification accuracies for the three ripeness grades (i.e., 'Green/					2015	[Zhu et al., 2015]

(*continued on next page*)

Table 2 (*continued*)

Quality parameter	Equipment	n	R^2c	RMSEC	R^2p	RMSEP or SEP	SDR	Year	Reference
			Break' 'Turning/Pink', and 'Light-red/Red')						
Quality assessment		165	a* and a*/b* = 0,74-0,80; SSC = 0.79; TA =0,72%; DM =0,45; Glucose = 0,61; Fructose = 0,43. citric acid = 0,50; malic acid =0,49	a* and a*/b* = 0.76–0.75; SSC = 0.75; TA= 0.69; DM=0.39; Glucose = 0.53; Fructose =0,36; citric acid =0,38; malic acid = 0,34		SEP a*and a*/b* = 2.58–0.09; SSC = 0.65%; TA = 0.06%; DM =0,33; Glucose = 4,2; Fructose = 4,1; citric acid = 0,62; malic acid = 0,22	a* and a*/b* = 1,97–2,23; SSC = 2,13; TA = 1,87; DM = 1,54; Glucose = 1,57; Fructose = 1,29; citric acid = 1,39; malic acid = 1,40	2015	[Torres et al., 2015]

For DM values, only the tomatoes from Santa Catarina differed statistically from the other states of origin. The values reported herein (4.66%–5.51%, Table 6) are similar to those (5.45 %–7.67 %) observed by Radzevičius et al. (2016) using NIR in intact tomato fruits.

3.3. Quimiometrics analysis

3.3.1. Principal component analysis – PCA

We did not observe any cluster of spectral information regarding the origin of the tomatoes for color parameters (Fig. 5), titratable acidity (Fig. 6a), or dry matter (Fig. 6b). Similar results were reported by Brito et al. (2021) regarding soluble solid content in salad tomatoes using a portable Vis-NIR spectrometer.

PCA for color parameters CIE $L^*a^*b^*$ C^* and h° (Fig. 5), did not make any spectral distinction between the samples. In the PCA for the L* parameter, one principal component (PC1) accounted for 89 % of the variation (Fig. 5a), whereas for the C* parameter (Fig. 5b), hue angle (h°) (Fig. 5c), CIE a* color parameter (Fig. 5d), and CIE b* color parameter (Fig. 5e), 94 % of the variation was explained by two principal components.

For the TA values (Fig. 6a), one principal component (PC1) was correlated with 74 % of the variables, with two principal components representing 94 % of the analyzed variables. The variation related to dry matter content could also be explained by one principal component (PC1) of 74 % of the analyzed samples, totaling 94 % of the variation explained by only two principal components (Fig. 6b). PCA, a technique used for qualitative analysis (Beghi et al., 2018), did not show any qualitative distinction for these parameters among samples.

3.4. Pls

Regarding the calibration and prediction models, the best performance was obtained using the spectral ranges 396–1,131 and 729–975 nm, respectively, in which, the spectra of the analyzed samples showed peaks at wavelengths of 507, 630, 675, 981, and 1,068 nm. After the application of the first derivative, peaks were observed at 480, 666, and 954 nm (Fig. 4a), and after the OSC pre-processing, the spectra showed peaks at 543–566 and 753–1,092 nm (Fig. 3c). Chlorophyll, lycopene, and water molecules are characterized by peaks at 575, 675, and 840−960 nm, respectively, and are important compounds in the evolution of color, TA content, and dry matter, respectively. Chlorophyll, is characterized by peaks in the region of 575 nm, lycopene at 675 nm, and water molecules in the region between 840 and 960 nm (Acharya et al., 2017). These are important compounds in the evaluation of color, TA content, and dry matter, respectively. Thus, the models that achieved the best performance (Table 7) were those developed with the complete wavelength (396–1,131 nm), in the near-infrared region (729–975 nm), the spectra in absorbance, a first derivative with 7 points (3 + 3), and OSC pre-processing.

3.4.1. Color

The models for the color parameters (CIE L*a*b*, C*, and h°) were developed with OSC pre-treatment, first derivative (3 + 3), and with spectra in absorbance, obtaining better results compared to the other attributes and with variations in R^2c from 0.52 to 0.94, and RMSEC from 1.79 to 5.54 for calibration models and R^2p from 0.39 to 0.94 for prediction models. The color parameter C*, which refers to saturation, showed satisfactory values in the prediction model, with an Rp^2 of 0.58, RMSEP of 2.1, and SDR equal to 1.55 (Fig. 7a). For the prediction of luminosity (L*) (Fig. 7b), the relationship between reference and predicted values obtained an Rp^2 value of 0.74, RMSEP of 2.44, and SDR equal to 1.93. These values were higher than those found by Ramos-Infante et al. (2019) when analyzing tomato quality characteristics, such as firmness, soluble solids content, and color CIE L* using Vis-NIR and hyperspectral imaging, which showed an R^2p value of 0.73 and an RMSEP value of 3.52.

Table 3
Systematic Bibliographic Review of works using near infrared spectroscopy (NIRS) to evaluate quality parameters in tomatoes fruit in the last 10 years (2016 – 2018).

Quality parameter	Equipment	n	R^2c	RMSEC	R^2p	RMSEP or SEP	SDR	Year	Reference
SSC, lycopene and titratable acidity	VIS/NIR spectroscopy (Avantes BV, Netherlands) (350-1050nm)	180	SSC (0,92), lycopene (0.84), TA (0,77)	SSC (0.271), lycopene (0.881) TA (0,008)	SCC (0,91), lycopene (0.84) TA (0,76)	RMSEP SCC (0.285), lycopene (0.913) TA (0.0084)		2016	[Saad et al., 2016]
SSC, dry matter and firmness	NIR spectrophotometer NIR Case NCS001A. Measurement (600–1000 nm)	2012 (96)	DM (0,9089), SSC (0,815) firmness (fruit 0,9119; skin 0,9624)					2016	[Radzevičius et al., 2016]
SSC, total acidity and ratio (SSC/AT)	USB4000 spectrometer (Ocean Optics USB4000) with fiber optic (IdopticsFIB-600-UV)	45	SSC =0,9841; TA =0,9751; ratio = 0,9674	SSC =0.0686 ; TA =0.2113; ratio = 0.0295	SSC =0.9727 ; TA =0.9501; ratio = 0.9253	RMSEP SSC =0.2295 ; TA =0.3312; ratio = 0.0539		2016	[Wang et al., 2016]
Soluble solids in two seasons (spring and summer)	MEMS - PHAZIR (NIR PHAZIR 1018, Anatec, Eke, Belgium)	144 (spring) 90 (summer)	spring = 0,8; summer = 0,9	spring = 0,2; summer = 0,1	spring= 0,8; summer = 0,6	RMSEP spring = 0,2; summer = 0,1	spring = 2,3; summer = 2,2	2016	[Camps et al., 2016]
Seeds viabillity	Hypersctral camera (Hyspex SWIR-384 Norsk Elektro Optikk, Norway)	1366	accuracy of cultivars 'Cal J', 'Chiuri', 'Monprecus' & 'NCL': 2013 (91, 98, 97 & 94%) 2014 (94, 83 & 73%) 2015 (100, 90 & 92%)					2016	[Shrestha et al., 2016]
Discrimination of tomato seeds cultivars	VideometerLab instrument (Videometer A/S, Hørsholm, Denmark).	1236 (viz. BL410, CL, Care Nepal, HRD17 & T9)	Accuracy range: 94 - 100%.					2016	[Shrestha et al., 2016]
Ripeness classification (PLS-DA)	FieldSpec® Pro FR portable spectrometer system (Analytical Spectral Devices, Inc., USA)	248	0.992	9.74	0.992	RMSEP 9.92		2017	[Lu et al., 2017]
Dry matter and color	"Nirvana" SWNIR spectrometer (equivalente ao F7-50, Felix Instruments, WA, USA)	100			DM = 0,92; CIE a* =0,95	RMSEP DM = 0,46; CIE a* =3,02	DM = 2,88; CIE a* = 5,18	2017	[Acharya et al., 2017]
Viability of tomato seeds	XD spectrophotometer (Foss-NIRSystems, Silver Spring, MD, USA)	268 (cal) 100 (val)	0,9446		0,939	SEP 6,57	3,96	2017	[Lee et al., 2017]
Separation of viable and non-viable tomatoes seeds	QIA1250 Fiberinterface to FT-NIR Analyser (Q-Interline A/S, QFAflex 600F, Tølløse, Denmark)	17 non-viable and 183 viable	14 out of 17 non-viable; 172 out of 183 viables					2017	[Shrestha et al., 2017]
Carotenoids compounds (ß-carotene, 5-cis lycopene, 13-cis lycopene, 9-cis lycopene, all-trans lycopene, zeaxanthin, lycoxanthin	Portable spectro-radiometer (FieldSpecHandHeld 2™, Analytical Spectral Devices (ASD), Inc., Boulder, USA) 325–1075 nm	100	ß-carotene (0,91), 5-cis lycopene (0,82), 13-cis lycopene (0,88), 9-cis lycopene (0,88), all-trans lycopene (0,72), zeaxanthin	ß-carotene (15,47), 5-cis lycopene (2,66), 13-cis lycopene (13,10), 9-cis lycopene (5,12), all-trans lycopene (255,31), zeaxanthin	ß-carotene (0,88), 5-cis lycopene (0,80), 13-cis lycopene (0,83), 9-cis lycopene (0,86), all-trans lycopene (0,70), zeaxanthin	RMSEP ß-carotene (17,69), 5-cis lycopene (3,098), 13-cis lycopene (15,06), 9-cis lycopene (5,97), all-trans lycopene (282,17),		2017	[Saad et al., 2017]

(*continued on next page*)

Table 3 (*continued*)

Quality parameter	Equipment	n	R^2c	RMSEC	R^2p	RMSEP or SEP	SDR	Year	Reference
and total carotenoids)			(0,83), lycoxanthin (0,35), total carotenoids (0,85)	(2,87), lycoxanthin (11,53), total carotenoids (284,94)	(0,80), lycoxanthin (0,20), total carotenoids (0,84)	zeaxanthin (3,28), lycoxanthin (12,93), total carotenoids (315,83)			
Local and global elasticity and SSC of two cherry tomato varieties and a grape tomato let in shelf-life for two weeks have been monitored.	non-destructive FT-NIR measurement		0,70 - 0,97				1.8 - 6.1	2017	[Camps & Gilli, 2017]
Texture, ph, SSC, color (C* and h°)	Bench spectrometer (MCS 600, CarlZeiss, Oberkochen, Germany) Vis-NIR 450–950 nm; NIR 950–1650 nm	205	SSC = 0,81; Color C* = 0,87; texture = 0,76; color h°= 0,92	SSC = 0,38; Color C*= 1,13; texture = 7,14; color h° = 1,27			SSC = 2,07; Color C* = 2,65; texture = 1,75; color h° = 3,46	2018	[Beghi et al., 2018]
Lycopene, β-Carotene, Phytoene, Phytofluene (μg. G-1)	Perten DA7200 NIR analyser (Perten Instruments, Huddinge, Sweden) equipped with a diode array detector (950-1650 nm wavelength range).	(80 Exocarp, 80 Mesocarp, 80 Endocarp and 80 tomato pomace) cal 240 val 80	Lycopene 0,95; β-Carotene, 0,91; Phytoene 0,94; Phytofluen 10,95	Lycopene 147,63; β-Carotene 16,65; Phytoene: 39,14; Phytofluene 18,52	Lycopene 0,95; β-Carotene 0,91; Phytoene 0,93; Phytofluene 0,94		Lycopene 4,81; β-Carotene 3,17; Phytoene 3,97; Phytofluene 4,09	2018	[Ibrahim et al., 2018]
TA, pH, total soluble solids	Portable spectrometer (AvaSpec- ULS 2048, Avantes, Eerbeek, and the Netherlands)	138	pH 0,94; TSS 0,94; TA 0,91	pH 0,009;TSS 0,03; TA 0,04				2018	[Sohrabi et al., 2018]
Soluble solids content and pH	Portable (Vis/SWNIR) spectrometer (400–1100 nm) (LOE-USB, tec5USA Inc., Plainview, NY, USA) and spectrometer NIR (900–1300 nm) (NIR 512L-1.7T1, Control Development, Inc., South Bend, IN, USA)	600	SSC: Vis/SWNIR (0,858), NIR (0,847) pH: Vis/SWNIR (0,766), NIR (0,778)	SSC: Vis/SWNIR (0,33), NIR (0,34) pH: Vis/SWNIR (0,11), NIR (0,11)	SSC: Vis/SWNIR (0,729), NIR (0,815) pH: Vis/SWNIR (0,743), NIR (0,741)	RMSEP SSC: Vis/SWNIR (0,45), NIR (0,37) pH: Vis/SWNIR (0,12), NIR (0,12)	SSC: Vis/SWNIR (1.41), NIR (1.72) pH: Vis/SWNIR (1.49), NIR (1.49)	2018	[Huang et al., 2018]
Firmness, SSC and pH	SRS system with a hyperspectral image equipment (Headwall Photonics, Inc., Fitchburg, MA, USA)	600			Firmness: optical absorption (OA): 0,876/ scattering (S): 0,420; SSC: 0,621 (OA)/ 0,435 (S); pH: 0,737 (OA)/ 0,413 (S)	RMSEP Firmness: (OA): 4,59/ (S): 8,5; SSC: 0,50 (OA)/ 0,57 (S); pH: 0,13 (OA)/ 0,17 (S)		2018	[Huang et al., 2018]
Firmness parameters: impact, compression area, and punction	Portable Vis/SWNIR spectrometer (Modelo LOE-USB, tec5USA Inc., Plainview, NY, 123 USA) - 400-1.100 nm and portable NIR spectrometer (Modelo NIR 512L-1.7T1, Control Development Inc., South Bend, IN, USA)- 900-1.700 nm	600	Vis/SWNIR: 0,899, 0,924, 0,938 (impact, compression area, and punction); NIR: 0,913 0,871, 0,911 (impact, compression area, and punction)	Vis/SWNIR: 5,432 1,893, 0,562 (impact, compression area, and punction); NIR: 5,068 2,431, 0,670 (impact, compression area, and punction)	Vis/SWNIR: 0.899, 0.917, 0.935 (impact, compression area, and punction); NIR: 0.846, 0.831, 0.853 (impact, compression area, and punction)	RMSEP Vis/SWNIR: 5,414 1,897, 0,578 (impact, compression area, and punction); NIR: 6,547 2,690, 0,856 (impact, compression area, and punction)		2018	[Huang et al., 2018]
Lycopene and β-carotene	spectrometer VIS/NIR (Life & Tech, CO, Ltd, Yongin, Korea) 500-110nm	244	Lycopene: 0,89; β-carotene: 0,88	Lycopene: 1,56; β-carotene: 0,63	Lycopene: 0,85; β-carotene: 0,77	RMSEP Lycopene: 1,79; β-carotene: 1,00		2018	[Tilahun et al., 2018]

Table 4
Systematic Bibliographic Review of works using near infrared spectroscopy (NIRS) to evaluate quality parameters in tomatoes fruit in the last 10 years (2019-2021).

Quality parameter	Equipment	n	R^2c	RMSEC	R^2p	RMSEP or SEP	SDR	Year	Reference
Firmness, Soluble solids and pH	Spectrometer NIR portable (950–1650 nm) Isuzu Optics Corp., China.	90			Firmness (0,9170) SSC (0,8596)and pH (0,8096)	RMSEP Firmness (0,5267) SSC (0,2010) and pH (0,0196)	Firmness (3.3466) SSC (2.6781) and pH (2.2932)	2019	[Feng et al., 2019]
SSC, Fructose, Glucose, citric acid, malic and glutamic acids	Spectrometer NIR portable (Ocean Optics, Dunedin, FL, USA) with detector In- GaAs (902-2094 nm)	5 butches with, 180, 168, 106, 108 and 88 samples each	SSC = 0.92; Fructose =0,93; Glucose =0,91; citric acid = 0,94; malic =0,96; glutamic = 0,94	SSC = 0.07; Fructose =0,64; Glucose =0,8; citric acid = 0,19; malic =0,10; glutamic = 0,51	SSC = 0.92; Fructose =0.82; Glucose =0,91; citric acid = 0,88; malic =0,90; glutamic = 0,81	RMSEP SSC = 0.14; Fructose =1,15; Glucose =1,49; citric acid= 0,31; malic =0,15; glutamic = 0,16	SSC = 3,81; Fructose =2,47; Glucose =2,3; citric acid = 2,85; malic =3,03; glutamic = 2,77	2019	[Ibáñez et al., 2019]
SSC and lycopene at different temperatures	Spectrometer portable (NIR0 developed by the authors	120			SSC 20°C = 0,8988; lycopene 20°C = 0,8023	RMSEP SSC 20°C = 0,292; lycopene 20°C = 7,45		2019	[Sheng et al., 2019]
Dry matter, SSC, firmness	hand-held spectrometer developed by the authors, with a DLP NIRscan nano Module (Texas Inst., Dallas, Texas)	experiment 1 (40 cherry tomatoes and 40 salad tomatoes) Experiment 2 (60 cherry tomatoes and 60 salad tomatoes) 3 exp (320 salad tomatoes and 360 cherry tomatoes)				RMSEP Firmness salad: 0,52 and 0,5 cherry; DM salad: 0,5 DM cherry: 0,52; SSC salad: 0,56 SSC cherry: 0,68		2019	[Goisser et al., 2019]
SSC, firmness, pH and color	Hyperspectral Vis-NIR camera (Fx10e, Specim, Oulu, Finland) 400-1000 nm	98			SSC = 0,96; firmness = 0,86; pH =0,92 and color L* = 0,73	RMSEP SSC = 0,11; firmness = 0,10; pH =0,02 and color L* = 3,523	SSC = 5,77; firmness= 3,13; pH =4,21 and color L* = 2,1	2019	[Ramos-Infante et al., 2019]
Fresh weight, pH, dry matter, color (L*a*b*), eletric condutivity, titrable acidity and SSC	Portable spectrometer (MicroNIR 1700 by Viavi Solutions® working between 908 and 1650 nm)	300	fresh weight: 0,57; color L*:0,44 a*: 0,38 b*:0,49; EC: 0,41 DM: 0,64; SSC 0,57; TA 0,57; pH 0,53	fresh weight: 0,74; color L*:0,82 a*: 0,92 b*:0,78; EC: 0,85 DM: 0,69; SSC 0,85; TA 0,75; pH 0,77				2019	[Castrignanò et al., 2019]
Soluble solids content and lycopene content	Portable NIR spectrometer (designed for this study): A miniature NIR spectrometer (digital light processing (DLP) NIR scan Nano; Texas Instruments) was combined with an android phone, to communicate wirelessly via BLE	176 cal and 15 val	SSC 0,93; lycopene 0,86	SSC 0,25; lycopene 6,38	SSC 0.8988; lycopene 0.8023	RMSEP SSC 0.292; lycopene 7.45		2019	[Sheng et al., 2019]
Lycopene and β-carotene	Remote sensing portable spectroradiometer RS-3500 (Ltd. Spectral Evolution).	432	lycopene |r| = 0.864; β-carotene (|r| = 0.682)		lycopene R^2 = 0.889; β-carotene R^2 = 0.553			2019	[Alsina et al., 2019]
SSC, TA, Glucose, Fructose, ascorbic acid and citric acid	Cary 630 portable (Agilent technologies Inc., Santa Clara, CA) and Agilent 4500 portable	681	SSC (0,99), TA (0,98), Glucose (0,99), Fructose (0,99),ascorbic acid (0,91), citric acid (0,96)		SSC (0,99), TA (0,98), Glucose (0,99), Fructose (0,99), ascorbic acid (0,94), citric acid (0,95)	SEP SSC (0,11), TA (0,03), Glucose (0,06), Fructose (0,06),ascorbic acid (3,34), citric acid (0,05)	SSC (9,6), TA (4,1), Glucose (8,2), Fructose (6,2), ascorbic acid (2,3), citric acid (3,0)	2020	[Akpolat et al., 2020]

(*continued on next page*)

Table 4 (*continued*)

Quality parameter	Equipment	n	R^2c	RMSEC	R^2p	RMSEP or SEP	SDR	Year	Reference
Detection and Quantitative Severity Stage Classification of Tomato Chlorosis Virus (tocv)	Portable spectrometer Unispec-SC (PP Systems, Inc.) 310-1100nm.	156 tomatoes plants, being 132 infected and 24 for control	Accuracy by XY-fusion network (88,3%) and multilayer perceptron with automated relevance determination (MLP–ARD) (92,1%)					2020	[Morellos et al., 2020]
Flesh firmness, lycopene (Lyco), b-carotene (b-Car), total phenolic content (TPC), and total flavonoid content (TFC)	F-750, Produce Quality Mater, Felix Instruments, Camas WA, USA), at wavelength range (285–1200 nm).	200 (50 em 4x)	0.966 for TPC, 0.959 for lyco, 0.984 for TFC, 0.938 for b-Car; and 0.919 for flesh firmness	firmness: 0.462, lycopene: 1.770, b-carotene: 0.163; TPC: 2.506 and TFC: 1.541				2020	[Alenazi et al., 2020]
Color (L*a*b* C h°), firmness, dry matter, TSS, Acidity, ratio brix/acid	F-750, SCiO and H-100F	color: 365; firmness: 365; DM: 160; TSS: 285; acidity: 285; ratio: 285	F-750: color (L*: 0,90; a*: 0,97; b*: 0,68; C*: 0,75; h°: 0,96) firmness: 0,93; DM: 0,96; TSS: 0,94; acidity: 0,74; ratio 0,74. SCiO: color (L*: 0,90; a*: 0,92; b*: 0,73; C*: 0,83; h°: 0,92) firmness: 0,89; DM: 0,97; TSS: 0,96; acidity: 0,66; ratio 0,70. H-100F: color (L*: 0,93; a*: 0,96; b*: 0,78; C*: 0,82; h°: 0,95) firmness: 0,92; DM: 0,96; TSS: 0,97; acidity: 0,82; ratio 0,77.	F-750: color (L*: 1,70; a*: 2,44; b*: 1,45; C*: 3,04; h°: 4,52) firmness: 5,17; DM: 0,33; TSS: 0,46; acidity: 0,67; ratio 2,11. SCiO: color (L*: 1,74; a*: 3,71; b*: 1,35; C*:2,54; h°: 6,50) firmness: 6,55; DM: 0,32; TSS: 0,35; acidity: 0,78; ratio 2,25. H-100F: color (L*: 1,39; a*: 2,65; b*: 1,22; C*:2,58; h°: 4,86) firmness: 5,35; DM: 0,35; TSS:0,32; acidity: 0,57; ratio1,96.				2020	[Goisser et al., 2020a]
Lycopene	F-750 Produce Quality Meter (λ = 477–1059 nm) H-100F (λ = 650–950 nm) and SCiO™ Molecular Sensor (λ = 740–1070 nm)	165	F-750 Produce Quality Meter (λ = 477–1059 nm) 0.96 H-100F (λ = 650–950 nm) 0,95 SCiO™ Molecular Sensor (λ = 740–1070 nm) 0,94	F-750 Produce Quality Meter (λ = 477–1059 nm) 12.06 H-100F (λ = 650–950 nm) 13.87 SCiO™ Molecular Sensor (λ = 740–1070 nm) 15.28				2020	[Goisser et al., 2020b]
Phenotyping (traits ph, °brix and carotenoids concentration)	Portable Vis-NIR spectrometer F-750 Felix instruments	473	0,29 pH 0,55 brix 0,20 carotenoids		ph 0,17 brix 0,32 carotenoids 0,17	SEP pH 0,09 brix 0,47 carotenoids 16,40	pH 1,08 brix 1,17 carotenoids 1,1	2020	[Kaur et al., 2020]
SSC	Portable Vis/NIR device (fibre optic probe, a spectrometer, a switch system, a microcontroller, and a power supply unit). The spectrometer (USB2000þ, Ocean Optics, Largo, FL,	168	0.831	0.189	0.820	RMSEP 0.207	1.75	2021	[Zhang et al., 2021]

(*continued on next page*)

Table 4 (*continued*)

Quality parameter	Equipment	n	R^2c	RMSEC	R^2p	RMSEP or SEP	SDR	Year	Reference
	USA) is equipped with a 2048-element CCD (ILX511, Sony, Minato, Tokyo, Japan) covering the spectral range of 200e1100 nm								
SSC	Portable Vis-NIR spectrometer F-750 Felix instruments	1706	0,65	0,3	0.67%	RMSEP 0,32	1,73	2021	[Brito et al., 2021]
TSS °brix, TA (g citric acid. 100 g−1), glucose (g. 100 g−1), frutose (g. 100 g−1), ascorbic (mg. 100 g−1) and citric acids (g. 100 g−1)	Portable NIR spectrometer (Neospectra-Module, Si-Ware Systems, Cairo, Egypt) based in a micro-electro-mechanical system spectrometer	319	SSC: 0,89; glucose: 0,87; fructose: 0,87; TA: 0,92; ascorbic acid: 0,82; citric acid: 0,87		SSC: 0,88; glucose: 0,83; fructose: 0,87; TA: 0,94; ascorbic acid: 0,81; citric acid: 0,86	SEP SSC: 0,52; glucose: 2,91; fructose: 2,83; TA: 0,04; ascorbic acid: 4,09; citric acid: 0,07		2021	[Borba et al., 2021]
Chemical parameters (DM, SSC, glucose, and fructose) and sensory attributes (sweetness, acidity, taste intensity, odor intensity, skin perception, mealiness, firmness, juiciness, and explosiveness)	FOSS NIR spectrometer system model 5000 (FOSS, Hilleroed, Denmark), Tomato juice spectra were acquired in transflectance method with a Rapid Content Analyzer (RCA) accessory and also using a gold transflector, which doubles the optical pathway. Tomato puree spectra were acquired in reflectance method with an OptiProbe Analyzer (FOSS, Hilleroed, Denmark)	60	fructose (juice): 0,98; glucose (juice): 0,97; fructose (puree): 0,96; glucose (puree): 0,96; SS (puree): 0,96; DM (puree): 0,95. sweetness: 0,71, acidity: 0,33, taste intensity: 0,34, odor intensity: 0,64, skin perception: 0,53, mealiness: 0,56, firmness: 0,33, juiciness: 0,68, and explosiveness: 0,68	fructose (juice): 0,33; glucose (juice): 0,45; fructose (puree): 0,13; glucose (puree): 0,12; SS (puree): 0,29; DM (puree):0,36. sweetness: 0,99, acidity: 1,53, taste intensity: 1,12, odor intensity: 1,28, skin perception: 1,21, mealiness: 0,93, firmness: 1,82, juiciness: 0,34, and explosiveness: 0,33	fructose (juice): 0,97; glucose (juice): 0,97; fructose (puree): 0,98; glucose (puree): 0,98; SS (puree): 0,97; DM (puree): 0,98. sweetness: 0,92, acidity: 0,70, taste intensity:0,76, odor intensity: 0,87, skin perception: 0,01, mealiness: 0,72, firmness: 0,38, juiciness: 0,66, and explosiveness: 0,85	RMSEP fructose (juice): 0,44; glucose (juice): 0,45; fructose (puree): 0,08; glucose (puree): 0,09; SS (puree): 0,24; DM (puree): 0,26. sweetness: 0,56, acidity: 0,97, taste intensity: 0,67, odor intensity: 0,77, skin perception: 0,94, mealiness: 0,65, firmness: 2,17, juiciness: 0,41, and explosiveness: 0,23	fructose (juice): 5,7; glucose (juice): 5,9; fructose (puree): 4,0; glucose (puree): 4,5; SS (puree): 3,9; DM (puree): 3,5. sweetness: 3,5, acidity: 1,7, taste intensity: 1,6, odor intensity: 2,8, skin perception: 0,6, mealiness: 1,8, firmness: 0,5, juiciness: 1,6, and explosiveness: 2,6	2021	[Sun et al., 2021]
Profenofos (mg/kg)	PS-100 spectroradiometer (Apogee Instruments, INC., Logan, UT, USA) with CCD detector, 2048 pixels, 1 nm resolution and halogen-tungsten light source in the wavelength range of 350–1100 nm	180	PLS 0.79; PCA-PLS 0.88; SPA-PLS 0.89; RF-PLS 0.91; ANN 0.86; PCA-ANN 0.93; SPA-ANN 0.98; RF-ANN 0.91	PLS: 0.66; PCA-PLS 0.53 SPA-PLS 0.46 RF-PLS 0.40 ANN 0.52 PCA-ANN 0.36 SPA-ANN 0.14 RF-ANN 0.40	PLS 0.85 PCA-PLS 0.85 SPA-PLS 0.80 RF-PLS 0.91 ANN 0.81 PCA-ANN 0.89 SPA-ANN 0.98 RF-ANN 0.89	PLS 0.62 PCA-PLS 0.55 SPA-PLS 0.59 RF-PLS 0.36 ANN 0.56 PCA-ANN 0.40 SPA-ANN 0.16 RF-ANN0.54		2021	[Nazarloo et al., 2021]
pH	Flame-T-VIS-NIR spectrometer (Ocean Optics, USA), with tungsten halogen lamp (HL-2000-HP-FHSA Ocean Optics, USA) as a light source, reflection probe (QR400-7-VIS-NIR Ocean Optics, USA)	99 (50 cal 49 val)	0,9			SEP 0,11	1,17	2021	[Wati et al., 2021]
SSC and maturity levels (green, turning, pink,	Transmittance spectrum	250	SCC 0.85; maturity levels % accuracy	SSC 0.26	SSC 0.73; maturity levels %accuracy	RMSEP SSC 0.27	SSC 1.44	2021	[Huang et al., 2021]

(*continued on next page*)

Table 4 (*continued*)

Quality parameter	Equipment	n	R^2c	RMSEC	R^2p	RMSEP or SEP	SDR	Year	Reference
light red and red)	measurement system (covering 600–1160 nm with spectral interval of 0.5 nm, model AvaSpec-ULS2048XL-EVO, Inc., Apeldoorn, Netherlands) and an industrial personal computer.		(Total 85.54 Green 97.31 Turning 86.03 Pink 72.18 Light Red 84.36 Red 94.74)		(Total 81.00 Green 95.77 Turning 83.38 Pink 68.46 Light Red 78.85 Red 91.15)				

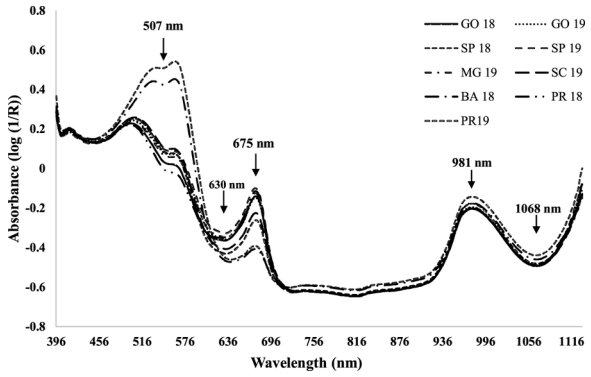

Fig. 2. Spectra in absorbance in the Vis-NIR region of intact tomatoes from six states and two seasons (2018 – 2019).

The PLSR model of prediction of the values of color parameter h° which refers to fruit tone, obtained an Rp^2 value of 0.89 and an SDR value of 3.06 (Fig. 7c). For the values of the color parameter a* corresponding to the variation of the red/green tone, the prediction model yielded an SDR value of 4.11, implying a model capable of accurate prediction (Nicolai et al., 2007), and an Rp^2 value of 0.94 (Fig. 7d). The results obtained for color parameters in this study were higher than those reported by Camps, Simone, & Gilli (2012), with an R^2 of 0.92 for parameter CIE a*, and those by Torres et al. (2015), which showed Rp^2 values for CIE a* and SDR of 0.76 and 1.97, respectively. Although the values of R^2 and SDR were lower than those found by Acharya et al. (2017), the RMSEP value obtained in this study was lower (2.89) than the RMSEP of 3.02 reported by these authors.

Finally, the prediction model for the color parameter b*, which refers to the variation in the yellow/blue tone, obtained the lowest results in relation to the other color parameters analyzed, with an Rp^2 equal to 0.39 and an SDR of 1.28. According to these data, the prediction models that obtained the values closest to the regression line were those related to hue angle (h°) (Fig. 7c) and CIE a* (Fig. 7d), thus presenting the highest accuracy in the prediction. Given the satisfactory performance of the models based on VIS-NIR instruments, especially parameter CIE a* used in the evaluation of most color indices for tomatoes, it is evident that they can be useful in the evaluation of tomato maturity and the resulting classification of the fruit.

3.4.2. *Titratable acidity*

For TA reference values, the models that yielded adequate results were developed with OSC pre-treatment, yet the predicted values obtained were low, with an Rp^2 of 0.25 and an RMSECV of 0.07 % (Fig. 8). These results are not satisfactory, as they showed that the model cannot accurately predict TA values. According to Walsh et al. (2020), given this RMSEP value, a reliable direct assessment of acidity in fruits with lower levels of acidity is unlikely, whereby, indirect assessment of acidity may be required; for example, an indirect assessment of chlorophyll level, which involves a correlation of acidity level with chlorophyll level, assessable through Vis-NIRS.

The absorption bands in the NIR region are complex because of the overlapping bands that hinder the interpretation of the relationship between the spectra and parameters of interest. In most fruits, acidity is a micro-constituent, making it difficult to analyze (Walsh et al., 2020; Borba et al., 2021). Thus, the relatively lower R^2 values for TA are likely related to the covalent bond between carbon and oxygen in the acid functional group (—COOH), with lower absorbance in relation to CH and O—H bonds (Cayuela, 2008; Chen, 2008).

3.4.3. *Dry matter*

The models for dry matter values were developed with OSC pre-treatment, showing satisfactory results, even though the Rc^2 and Rp^2 results were less than 0.7 (0.62 and 0.59, respectively), due to the low RMSEC (0.48 %) and RMSEP (0.68 %) in the prediction of reference values (Fig. 9), meaning that the range of error in predicting the dry matter values are lower than 1%. These values were stronger than those reported by Torres et al. (2015), who reported an R_c^2 value of 0.45 % and a coefficient of prediction of 0.39 %.

However, due to the low values of standard deviation of the samples, the results obtained in this study were lower than the values obtained by Acharya et al. (2017), who reported R^2 ranging from 0.90 to 0.93 and an RMSECV < 0.5 %. According to Torres et al. (2015), to raise a low prediction value, the standard deviation of the samples analyzed should be increased, thereby improving the predictive capacity of the models.

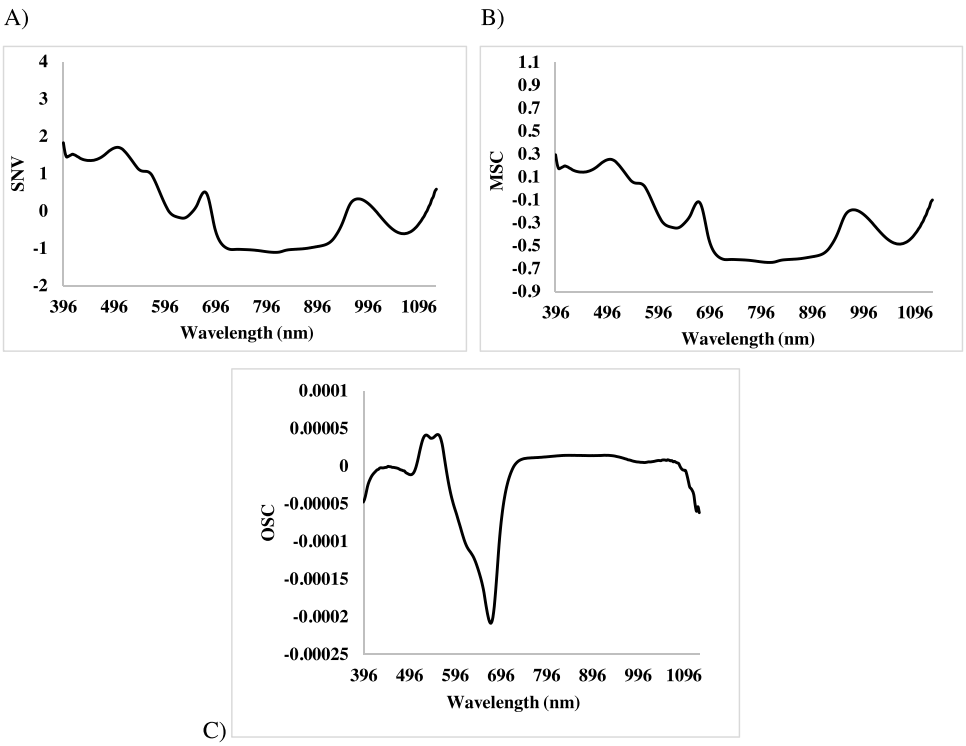

Fig. 3. Mean of spectra in the Vis-NIR region after SNV (A), MSC (B) e OSC (C) pre-processing of intact tomatoes from six states and two seasons (2018 – 2019).

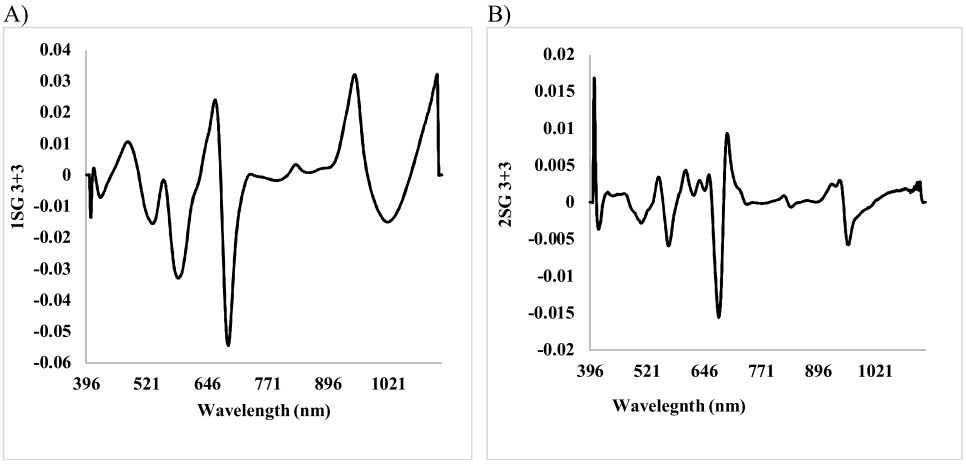

Fig. 4. Mean of spectra in the Vis-NIR region after Savitzky-Golay first derivative (A) and Saviztky-Golay second derivative (B) of intact tomatoes from six states and two seasons (2018 – 2019).

Table 5
Analysis of Variance (ANOVA) of the color parameters *CIE L*a*b**, C (chroma) e h° (hue anlge) means of the analyzed tomatoes, identified according to the state of origin: Goiás (GO), Minas Gerais (MG), Paraná (PA), Santa Catarina (SC) and São Paulo (SP). 1 – Means followed by the same letter in the same column do not differ statistically among themselves by Tukey test ($p < 0.05$); 2 – coefficient of variation.

	COLOR PARAMETER				
STATE	L*	a*	b*	C*	h°
GO	48,97b[1]	4,69a	29,46b	32,07a	82,71b
MG	46,57ab	10,03ab	28,20ab	31,27a	70,82ab
PR	39,32a	21,23c	24,07ab	32,16a	48,76a
SC	47,33b	6,89a	26,88ab	28,33a	76,32b
SP	41,43ab	18,89bc	22,53a	29,44a	50,08a
CV (%)[2]	20,11	205,79	28,06	25,01	39,95

Table 6
Analysis of Variance (ANOVA) of the quality attributes (titratable acidity – TA and dry matter – DM) of the analyzed tomatoes, identified according to the state of origin: São Paulo (SP), Goiás (GO), Minas Gerais (MG), Santa Catarina (SC), Bahia (BA) and Paraná (PA). 1 – Means followed by the same letter in the same column do not differ statistically among themselves by Tukey test ($p < 0.05$); 2 - Coefficient of variation.

	QUALITY ATTRIBUTES (mean)	
STATES	TA (% citric acid)	DM (%)
GO	0.226868 a[1]	5.154083 a b
SP	0.265006 a b	4.667432 a
MG	0.232815 a	5.294538 a b
SC	0.213702 a	5.517321 b
PR	0.235628 a	5.146516 a b
BA	0,307070 b	
CV[2] (%)	34.28	18.45

This is useful for the tomato packaging industry, because the non-destructive determination of DM content is essential for fruit classification purposes, as it ensures that fruit lots are at similar levels of DM.

4. Conclusions

The use of a portable Vis-NIR spectrometer can be useful in predicting contents such as dry matter and color evaluation in intact tomatoes, allowing for classification. Thus, this study showed that the Vis-NIR technique applied with chemometric models can be used as a tool for the precise classification of intact tomato fruit, in terms of color and dry matter content. With the use of portable spectrometers, these classifications can be made in the field with a single piece of equipment in real-time, ensuring the high quality desired by consumers in tomatoes.

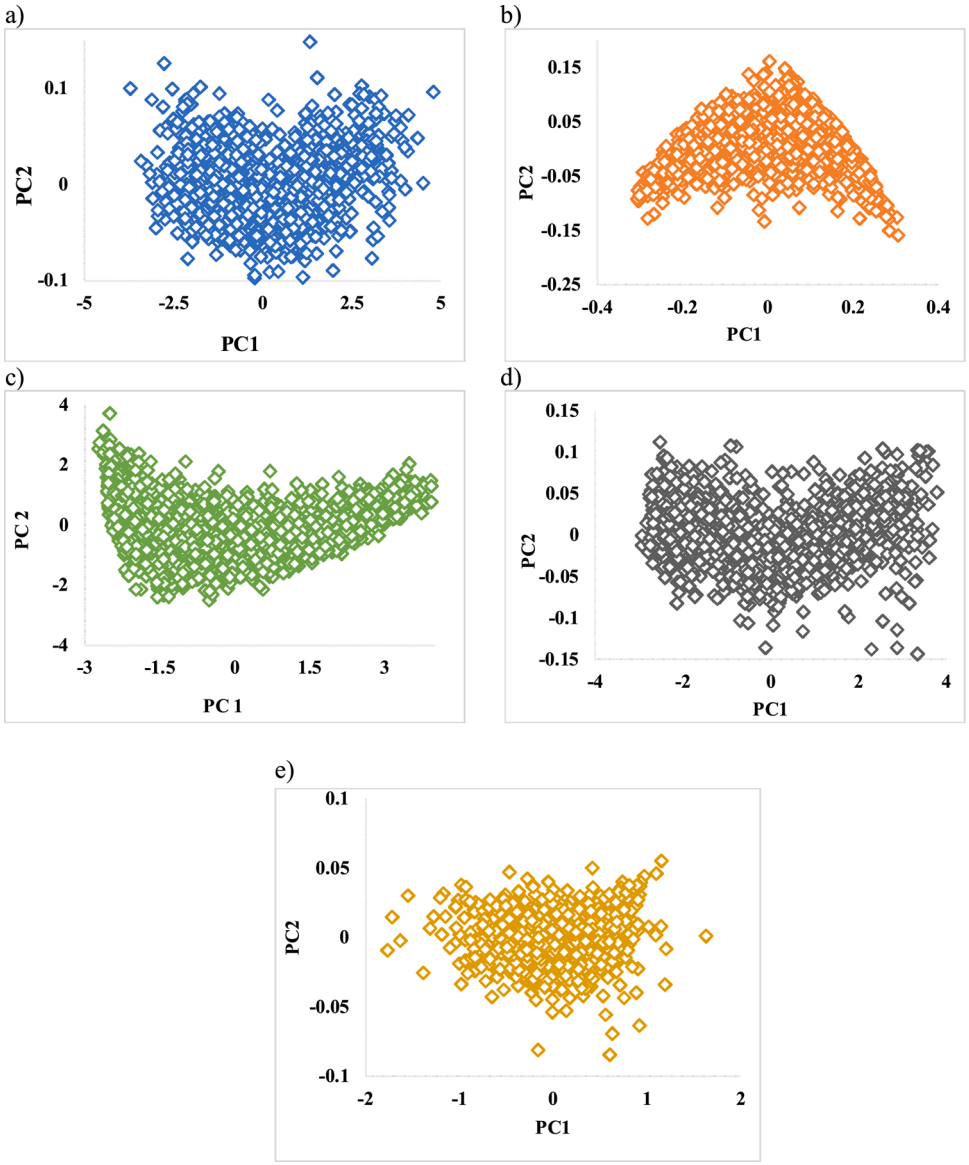

Fig. 5. Principal Component Analysis (PCA) of the color parameters reference values CIE L^* (a), C^* (b), hue angle (h°) (c), CIE a^* (d), and CIE b^* (e) for the populations POP1 and POP2 in 2019.

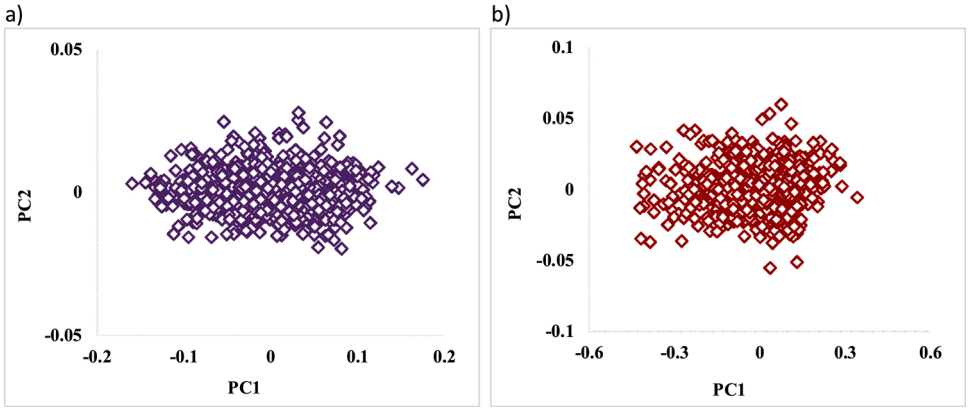

Fig. 6. Principal Component Analysis (PCA) of titratable acidity (TA) reference values in 2018 and 2019 (a) and of dry matter reference values in 2019 (b).

Table 7
Partial least squares regression results for the calibration and the prediction models for color parameters (L^*, C^*, a^*, b^* e h^*), titratable acidity (TA) and dry matter (DM).

			CALIBRATION						PREDICTION			
Attributes	Pre-processing	Wavelength range (nm)	P. C.[1]	R_c^2 [2]	R^2_{cv} [3]	RMESEC[4]	RMSECV[5]	$SDR_{(SD/RMSECV)}$[6]	R^2[7]	RMSEP[8]	SEP[9]	$SDR_{(SD/SEP)}$[10]
TA (% citric acid)	OSC	729–975	11	0,26	0,24	0,07	0,07	1,15	0,25	0,07	0,07	1,15
MS (%)	OSC	729–975	11	0,62	0,60	0,48	0,49	1,95	0,59	0,46	0,46	1,92
L^*	OSC	396–1131	3	0,77	0,77	2,57	2,60	2,07	0,74	2,44	2,43	1,93
a^*	OSC	396–1131	1	0,85	0,85	4,62	4,63	2,55	0,94	2,89	2,85	4,11
b^*	OSC	396–1131	4	0,52	0,50	3,14	3,20	1,42	0,39	2,91	2,91	1,28
C^*	1SG 3 + 3	396–1131	10	0,76	0,75	1,79	1,84	1,99	0,59	2,10	2,10	1,55
h	ABS	396–1131	1	0,94	0,94	5,54	5,55	4,01	0,89	7,41	7,38	3,06

[1] principal components.
[2] calibration coefficient.
[3] cross-validation coefficients.
[4] root mean square error calibration.
[5] root mean square error cross-validation.
[6] ratio (calibration standard deviation/RMSECV).
[7] prediction coefficient.
[8] root mean square error prediction.
[9] RMSEP corrected by bias.
[10] ratio (prediction standard deviation/SEP.

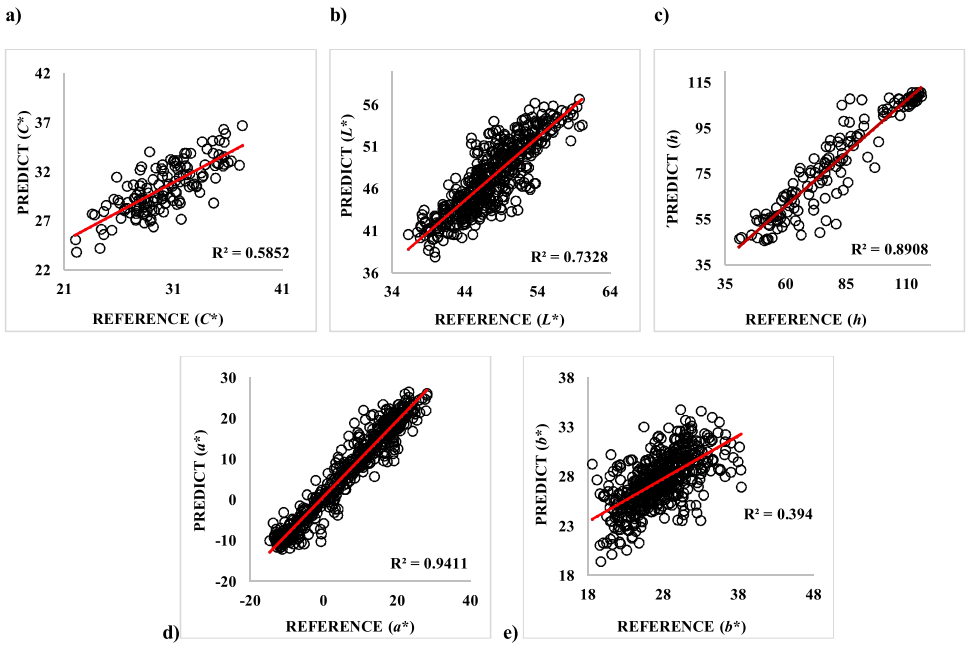

Fig. 7. Results of prediction values for color parameters of population POP2 based in the best PLSR models results in the wavelength 396-1131 nm, in which (a) CIE L* $Rp^2 = 0,74$, RMSEP = 2,44 and SEP = 2,43 with OSC pre-processing; (b) C* $Rp^2 = 0,59$, RMSEP = 2,10 and SEP = 2,10 with first derivative 3 + 3 pre-processing; (c) h°, with $Rp^2 = 0,89$, RMSEP = 7,41 and SEP = 7,38 with spectra in absorbance; (d) a^* with $Rp^2 = 0,94$, RMSEP = 2,89 and SEP = 2,85 with OSC pre-processing; and (e) b^* with $Rp^2 = 0,39$, RMSEP = 2,91 and SEP = 2,91 with OSC pre-processing.

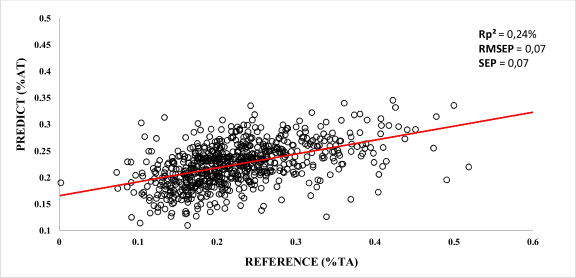

Fig. 8. Result of prediction values for titratable acidity (TA) reference values of prediction population POP3, based on the best PLSR model prediction at the wavelength 729-975 nm, with OSC pre-processing.

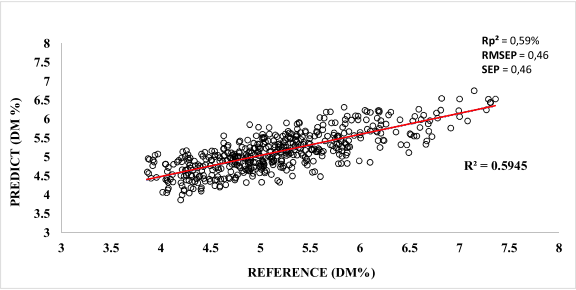

Fig. 9. Result of prediction values for dry matter (DM) reference values of prediction population POP2, based on the best PLSR model prediction at the wavelength 729-975 nm, with OSC pre-processing.

Author contributions

Annelisa Arruda de Brito: Conceptualization, Methodology, Software, Validation, Formal analysis, Investigation, Data Curation, Writing - Original Draft, Writing - Review & Editing, Project administration **Fernanda Campos**: Investigation, Data Curation **Abadia dos Reis Nascimento**: Resources, Funding acquisition. **Clarissa Damiani:** Resources, Funding acquisition. **Flávio Alves da Silva**: Writing - Review & Editing **Gustavo Henrique de Almeida Teixeira:** Conceptualization, Methodology, Writing - Review & Editing **Luis Carlos Cunha Júnior**: Conceptualization, Methodology, Software, Validation, Formal analysis, Resources, Writing - Review & Editing, Supervision, Project administration, Funding acquisition.

Declaration of Competing Interest

The authors declare that they have no known competing financial interests or personal relationships that could have appeared to influence the work reported in this paper.

Acknowledgements

The authors would like to acknowledge the financial support of the Coordenação de Aperfeiçoamento de Pessoal de Nível Superior - Brasil (CAPES) – Financial code 001, the Fundação de Apoio à Pesquisa do Estado de Goiás (FAPEG) (process no. 201510267001478), Ministério da Ciência, Tecnologia, Inovações e Comunicações (MCTIC), and Conselho Nacional de Desenvolvimento Científico e Tecnológico (CNPq) (process no. 406617/2018-0).

References

A.O.A.C. (Association of Official Analytical Chemists), 1997. In: Williams, Sidney (Ed.), Official Methods of Analysis, 16 ed., p. 1141 Arlington.

Acharya, U.K., Subedi, P.P., Walsh, K.B., 2017. Robustness of tomato quality evaluation using a portable Vis-SWNIRS for dry matter and colour. Int. J. Anal. Chem. https://doi.org/10.1155/2017/2863454.

Alenazi, M.M., Shafiq, M., Alsadon, A.A., Alhelal, I.M., Alhamdan, A.M., Solieman, T.H., Saad, M.A., 2020. Non-destructive assessment of flesh firmness and dietary antioxidants of greenhouse-grown tomato (Solanum lycopersicum L.) at different fruit maturity stages. Saudi J. Biol. Sci. 27 (10), 2839–2846.

Alsina, I., Dubova, L., Duma, M., Erdberga, I., Avotiņš, A., Rakutko, S., 2019. Comparison of lycopene and β-carotene content in tomatoes determined with chemical and non-destructive methods. https://doi.org/10.15159/ar.19.085.

Amodio, M., Ceglie, F., Chaudhry, M.m.a., Piazzolla, F., Colelli, G., 2017. Potential of NIR spectroscopy for predicting internal quality and discriminating among strawberry fruits from different production systems. Postharvest Biol. Technol. 125, 112–121.

Akpolat, H., Barineau, M., Jackson, K.A., Aykas, D.P., Rodriguez-Saona, L.E., 2020. Portable infrared sensing technology for phenotyping chemical traits in fresh market tomatoes. Lwt 124, 109164. https://doi.org/10.1016/j.lwt.2020.109164.

W.G. Berra , 2012; Visible/near infrared spectroscopic method for the prediction of lycopene in tomato (Lycopersicon esculentum, Mill.) Fruits. Science, Technology and Arts Research Journal, 1(3), 17-23. DOI:10.4314/star.v1i3.98795.

Batu, A., 2004. Determination of acceptable firmness and color values of tomatoes. J. Food Eng. 61 (3), 471–475.

Beghi, R., Buratti, S., Giovenzana, V., Benedetti, S., Guidetti, R., 2017. Electronic nose and visible-near infrared spectroscopy in fruit and vegetable monitoring. Rev. Anal. Chem. 36 (4).

Beghi, R., Giovenzana, V., Tugnolo, A., Guidetti, R., 2018. Application of visible/near infrared spectroscopy to quality control of fresh fruits and vegetables in large-scale mass distribution channels: a preliminary test on carrots and tomatoes. J. Sci. Food Agric. 98 (7), 2729–2734. https://doi.org/10.1002/jsfa.8768.

Blanco, M., Coello, J., Montoliu, I., Romero, Ma., 2001. Orthogonal signal correction in near infrared calibration. Anal. Chim. Acta.

Borba, K.R., Aykas, D.P., Milani, M.I., Colnago, L.A., Ferreira, M.D., Rodriguez-Saona, L. E., 2021. Portable near infrared spectroscopy as a tool for fresh tomato quality control analysis in the field. Appl. Sci. 11 (7), 3209. https://doi.org/10.3390/app11073209.

Brito, A.A., Campos, F., Dos Reis Nascimento, A., De Carvalho Corrêa, G., Da Silva, F.A., Teixeira, G.H.A., Cunha Júnior, L.C.C., 2021. Determination of soluble solid content in market tomatoes using near-infrared spectroscopy. Food Control 126, 108068. https://doi.org/10.1016/j.foodcont.2021.108068.

Camps, C., Simoné, C., Gilli, C., 2012. ASSESSMENT OF TOMATO QUALITY USING PORTABLE NIR SPECTROSCOPY AND PLSR WITH WAVELENGTHS SELECTION. Acta Horticulturae 936, 437–442. https://doi.org/10.17660/actahortic.2012.936.

Camps, C., Deltheil, L., Gilli, C., Carlen, C., 2016. Using the soluble solids accumulation in tomatoes from fruit setting until harvest for the construction of a predictive model by hand-held NIR Spectroscopy. Acta Horticulturae 1119, 321–328. https://doi.org/10.17660/actahortic.2016.1119.

Camps, C., Gilli, C., 2017. Prediction of local and global tomato texture and quality by FT-NIR spectroscopy and chemometric. Eur. J. Hortic. Sci 82 (3), 126–133. https://doi.org/10.17660/eJHS.2017/82.3.2.

Castrignanò, A., Buttafuoco, G., Malegori, C., Genorini, E., Iorio, R., Stipic, M., Venezia, A., 2019. Assessing the feasibility of a miniaturized near-infrared spectrometer in determining quality attributes of San Marzano tomato. Food Anal. Methods 12 (7), 1497–1510.

Cayuela, J.A., 2008. Vis/NIR soluble solids prediction in intact oranges (Citrus sinensis L.) cv. Valencia Late by reflectance. Postharvest Biol. Technol. 47, 75–80.

Chen, L., 2008. Non-destructive Measurement of Tomato Quality Using Visible and Near-infrared Reflectance Spectroscopy. MSc. Thesis. Department of Bio-resource Engineering, Macdonald Campus, McGill University, Canada.

Conzen, J.P., 2003. Multivariate Calibration, Bruker Optics.

Cortés, V., Blasco, J., Aleixos, N., Cubero, S., Talens, P., 2019. Monitoring strategies for quality control of agricultural products using visible and near-infrared spectroscopy: a review. Trends Food Sci. Technol.

Dubois, M., Gilles, K.A., Hamilton, J.K., Rebers, P.A., Smith, F., 1956. Colorimetric method for determination of sugars and related substances. Anal. Chem. Washington 28, 350–356.

Ecarnot, M., Bączyk, P., Tessarotto, L., Chervin, C., 2013. Rapid phenotyping of the tomato fruit model, Micro-Tom, with a portable VIS–NIR spectrometer. Plant Physiol. Biochem. 70, 159–163. https://doi.org/10.1016/j.plaphy.2013.05.019.

Escribano, S., Biasi, Wv, Lerud, R., Slaughter, Dc, Mitcham, Ej, 2017. Non-destructive prediction of soluble solids and dry matter content using NIR spectroscopy and its relationship with sensory quality in sweet cherries. Postharvest Biol. Technol. 128, 112–120.

Feng, L., Zhang, M., Adhikari, B., Guo, Z., 2019. Nondestructive detection of postharvest quality of cherry tomatoes using a portable NIR spectrometer and chemometric algorithms. Food Anal. Methods 12 (4), 914–925. https://doi.org/10.1007/s12161-018-01429-9.

Ferreira, S.M.R., Freitas, R.J.S.D., Lazzari, E.N., 2004. Padrão de identidade e qualidade do tomate (Lycopersicon esculentum Mill.) de mesa. Ciência Rural 34, 329–335.
Goisser, S., Fernandes, M., Wittmann, S., Ulrichs, C., Mempel, H., 2020a. Evaluating the practicability of commercial food-scanners for non-destructive quality assessment of tomato fruit. JOURNAL OF APPLIED BOTANY AND FOOD QUALITY 93, 204–214. https://doi.org/10.5073/JABFQ.2020.093.025.
Goisser, S., Wittmann, S., Fernandes, M., Mempel, H., Ulrichs, C., 2020b. Comparison of colorimeter and different portable food-scanners for non-destructive prediction of lycopene content in tomato fruit. Postharvest Biology and Technology 167, 111232. https://doi.org/10.1016/j.postharvbio.2020.111232.
Goisser, S., Krause, J., 2019. Fernandes M , Mempel H. Determination of tomato quality attributes using portable NIR-sensors. KIT Scientific Publishing. Mar 18.
GOLIC, M., WALSH, K.B., 2006. Robustness of calibration models based on near infrared spectroscopy for the in-line grading of stone fruit for total soluble solids content. Anal. Chim. Acta 555 (2), 286–291. https://doi.org/10.1016/j.aca.2005.09.014.
Gómez, A.H., He, Y., Pereira, A.G., 2006. Non-destructive measurement of acidity, soluble solids and firmness of Satsuma mandarin using Vis/NIR-spectroscopy techniques. J. Food Eng. 77 (2), 313–319. https://doi.org/10.1016/j.jfoodeng.2005.06.036.
Guthrie, J.A., Walsh, K.B., Reid, D.J., Liebenberg, C.J., 2005. Assessment of internal quality attributes of mandarin fruit. 1. NIR calibration model development. Aust. J. Agric. Res. 56 (4), 405. https://doi.org/10.1071/ar04257.
He, Y., Zhang, Y., Pereira, A.G., Gomez, A.H., Wang, J., 2005. Nondestructive determination of tomato fruit quality characteristics using vis/NIR spectroscopy technique. Int. J. Inf. Technol. 11, 97–108.
Huang, Y., Lu, R., Chen, K., 2018a. Assessment of tomato soluble solids content and pH by spatially-resolved and conventional Vis/NIR spectroscopy. J. Food Eng. 236, 19–28. https://doi.org/10.1016/j.jfoodeng.2018.05.008.
Huang, Y., Lu, R., Hu, D., Chen, K., 2018b. Quality assessment of tomato fruit by optical absorption and scattering properties. Postharvest Biology and Technology 143, 78–85. https://doi.org/10.1016/j.postharvbio.2018.04.016.
Huang, Y., Lu, R., Chen, K., 2018c. Prediction of firmness parameters of tomatoes by portable visible and near-infrared spectroscopy. Journal of food engineering 222, 185–198. https://doi.org/10.1016/j.jfoodeng.2017.11.030.
Huang, Y., Dong, W., Chen, Y., Wang, X., Luo, W., Zhan, B., Zhang, H., 2021. Online detection of soluble solids content and maturity of tomatoes using Vis/NIR full transmittance spectra. Chemometrics and Intelligent Laboratory Systems 210, 104243. https://doi.org/10.1016/j.chemolab.2021.104243.
Ibáñez, G., Cebolla-Cornejo, J., Martí, R., Roselló, S., Valcárcel, M., 2019. Non-destructive determination of taste-related compounds in tomato using NIR spectra. J. Food Eng. 263, 237–242. https://doi.org/10.1016/j.jfoodeng.2019.07.004.
Ibrahim, A., Daood, H., Bori, Z., Helyes, L., 2018. Using Infrared Spectroscopy for Tracking and Estimating Antioxidant in Tomato Fruit Fractions. European Journal of Engineering and Technology Research 3 (5), 21–30. https://doi.org/10.24018/ejers.2018.3.5.736.
INSKEEP, W.P., BLOOM, P.R., 1985. Extinction coefficients of chlorophyll *a* and *b* in N, N-Dimethylformamide and 80% acetone. Plant Physiol. Minneapolis 77, 483–485.
Kaur, A., Donis-Gonzalez, I.R., St. Clair, D.A., 2020. Evaluation of a hand-held spectrophotometer as an in-field phenotyping tool for tomato and pepper fruit quality. The Plant Phenome Journal 3 (1), e20008. https://doi.org/10.1002/ppj2.20008.
Kennard, R.W., Stone, L.A., 1969. Technometrics 11, 137–148.
Kim, D.Y., Cho, B.K., Mo, C.Y., Kim, Y.S., 2010. Study on prediction of internal quality of cherry tomato using Vis/NIR spectroscopy. Journal of Biosystems Engineering 35 (6), 450–457. https://doi.org/10.5307/JBE.2010.35.6.450.
Kim, G., Kim, D.Y., Kim, G.H., Cho, B.K., 2013. Applications of discrete wavelet analysis for predicting internal quality of cherry tomatoes using VIS/NIR spectroscopy. Journal of Biosystems Engineering 38 (1), 48–54. https://doi.org/10.5307/JBE.2013.38.1.048.
Lee, H.S., Jeon, Y.A., Lee, Y.Y., Lee, G.A., Raveendar, S., Ma, K.H., 2017. Large-scale screening of intact tomato seeds for viability using near infrared reflectance spectroscopy (NIRS). Sustainability 9 (4), 618. https://doi.org/10.3390/su9040618.
Lime, B.J., Griffiths, F.P., O'connor, R.T., Heinzelmann, D.C., Mccall, E.R., 1957. Spectrophotometric methods for determining pigmentation – beta-carotene and lycopene – in ruby red grapefruit. Agric. Food Chem. Easton 5 (12), 941–944.
López, C.A.F., Gómez, P.A., 2004. Comparison of color indexes for tomato ripening. Hortic. Bras. 22 (3), 534–537.
Lu, H., Wang, F., Liu, X., 2017. et al. Rapid Assessment of Tomato Ripeness Using Visible/Near-Infrared Spectroscopy and Machine Vision. Food Anal. Methods 10, 1721–1726. https://doi.org/10.1007/s12161-016-0734-9.
Magwaza, L.S., Opara, U.L., Nieuwoudt, H., Cronje, P.J., Saeys, W., Nicolaï, B., 2012. NIR spectroscopy applications for internal and external quality analysis of citrus fruit—a review. Food Bioproc. Tech. 5 (2), 425–444.
Mcguire, R.G., 1992. Reporting of objective color measurements. Hort Sci. 27 (12), 1254–1255.
Menezes, C.M., Da Costa, A.B., Renner, R.R., Bastos, L.F., Ferrao, M.F., Dresslere, V.L., 2014. Direct determination of tannins in *Acacia mearnsii* bark using near-infrared spectroscopy. Anal. Methods-UK 6 (20), 8299–8305.
Morais, C.L., Santos, M.C., Lima, K.M., Martin, F.L., 2019. Improving data splitting for classification applications in spectrochemical analyses employing a random-mutation Kennard-Stone algorithm approach. Bioinformatics 35 (24), 5257–5263.
Morellos, A., Tziotzios, G., Orfanidou, C., Pantazi, X.E., Sarantaris, C., Maliogka, V., Moshou, D., 2020. Non-Destructive Early Detection and Quantitative Severity Stage Classification of Tomato Chlorosis Virus (ToCV) Infection in Young Tomato Plants Using Vis?NIR Spectroscopy. Remote Sensing 12 (12), 1920. https://doi.org/10.3390/rs12121920.
Moretti, C.L., 2006. Protocolos de avaliação da qualidade química e física de tomate. Embrapa Hortaliças-Comunicado Técnico (INFOTECA-E).
Moretti, C.L., Sargent, S.A., Huber, D.J., Calbo, A.G., Puschmann, R., 1998. Chemical composition and physical properties of pericarp, locule and placental tissues of tomatoes with internal bruising. J. Am. Soc. Hortic. Sci. Alexandria 123 (4), 656–660.
Nazarloo, A.S., Sharabiani, V.R., Gilandeh, Y.A., Taghinezhad, E., Szymanek, M., 2021. Evaluation of Different Models for Non-Destructive Detection of Tomato Pesticide Residues Based on Near-Infrared Spectroscopy. Sensors 21 (9), 3032. https://doi.org/10.3390/s21093032.
Nicolai, B.M., Beullens, K., Bobelyn, E., Peirs, A., Saeys, W., Theron, K.I., Lammertyn, J., 2007. Nondestructive measurement of fruit and vegetable quality by means of NIR spectroscopy: a review. Postharvest Biol. Technol. 46 (2), 99–118. https://doi.org/10.1016/j.postharvbio.2007.06.024.
Oliveira, G.A., Bureau, S., Renard, C.M.G.C., Pereira-Netto, A.B., de Castilhos, F., 2014. Comparison of NIRS approach for prediction of internal quality traits in three fruit species. Food chemistry 143, 223–230. https://doi.org/10.1016/j.foodchem.2013.07.122.
Pasquini, C., 2003. Near infrared spectroscopy: fundamentals, practical aspects and analytical applications. J. Braz. Chem. Soc. 14, 198–219.
Porep, J.U., Kammerer, D.R., Carle, R., 2015. On-line application of near infrared (NIR) spectroscopy in food production. Trends Food Sci. Technol. 46 (2), 211–230.
Radzevičius, A., Viškelis, J., Karklelienė, R., Juškevičienė, D., Viškelis, P., 2016. Determination of tomato quality attributes using near infrared spectroscopy and reference analysis. Zemdirbyste-Agriculture 103 (1). https://doi.org/10.13080/z-a.2016.103.012.
Ramos-Infante, S.J., Suarez-Rubio, V., Luri-Esplandiu, P., Saiz-Abajo, M.J., 2019. Assessment of tomato quality characteristics using Vis/Nir hyperspectral imaging and chemometrics. 10th Workshop on Hyperspectral Imaging and Signal Processing: Evolution in Remote Sensing (WHISPERS). https://doi.org/10.1109/whispers.2019.8921170.
Saad, A.G., Jaiswal, P., Jha, S.N., 2014. Non-destructive quality evaluation of intact tomato using VIS-NIR spectroscopy. Int. J. Adv. Res. 2 (12), 632–639.
Saad, A., Jha, S.N., Jaiswal, P., Srivastava, N., Helyes, L., 2016. Non-destructive quality monitoring of stored tomatoes using VIS-NIR spectroscopy. Engineering in agriculture, environment and food 9 (2), 158–164. https://doi.org/10.1016/j.eaef.2015.10.004.
Saad, A.G., Pék, Z., Szuvandzsiev, P., Gehad, D.H., Helyes, L., 2017. (2017). Determination of carotenoids in tomato products using Vis/NIR spectroscopy. Journal of Microbiology. Biotechnology and Food Sciences 27–31. https://doi.org/10.15414/jmbfs.2017.7.1.27-31.
Savitzky, A., Golay, M.J.E., 1964. Smoothing and differentiation of data by simplified least squares procedures. Anal. Chem. 36, 1627–1639. https://doi.org/10.1021/ac60214a047.
Ścibisz, I., Reich, M., Bureau, S., Gouble, B., Causse, M., Bertrand, D., Renard, C.M., 2011. Mid-infrared spectroscopy as a tool for rapid determination of internal quality parameters in tomato. Food Chemistry 125 (4), 1390–1397. https://doi.org/10.1016/j.foodchem.2010.10.012.
Sheng, R., Cheng, W., Li, H., Ali, S., Agyekum, A.A., Chen, Q., 2019. Model development for soluble solids and lycopene contents of cherry tomato at different temperatures using near-infrared spectroscopy. Postharvest Biology and Technology 156, 110952. https://doi.org/10.1016/j.postharvbio.2019.110952.
Shrestha, S., Deleuran, L.C., Gislum, R., 2016a. Classification of different tomato seed cultivars by multispectral visible-near infrared spectroscopy and chemometrics. Journal of Spectral Imaging 5. https://doi.org/10.1255/jsi.2016.a1.
Shrestha, S., Knapič, M., Žibrat, U., Deleuran, L.C., Gislum, R., 2016b. Single seed near-infrared hyperspectral imaging in determining tomato (Solanum lycopersicum L.) seed quality in association with multivariate data analysis. Sensors and Actuators B: Chemical 237, 1027–1034. https://doi.org/10.1016/j.snb.2016.08.170.
Shrestha, S., Deleuran, L.C., Gislum, R., 2017. Separation of viable and non-viable tomato (Solanum lycopersicum L.) seeds using single seed near-infrared spectroscopy. Computers and Electronics in Agriculture 142, 348–355. https://doi.org/10.1016/j.compag.2017.09.004.
Sirisomboon, P., Tanaka, M., Kojima, T., Williams, P., 2012. Nondestructive estimation of maturity and textural properties on tomato 'Momotaro' by near infrared spectroscopy. J. Food Eng. 112 (3), 218–226, 10.1016/j.jfoodeng.2012.04.007.
Sohrabi, M.M., Ahmadi, E., Monavar, H.M., 2018. Nondestructive analysis of packaged grape tomatoes quality using PCA and PLS regression by means of fiber optic spectroscopy during storage. Food Measure 12, 949–966. https://doi.org/10.1007/s11694-017-9710-3.
Subedi, P.P., Walsh, K.B., 2020. Assessment of avocado fruit dry matter content using portable near infrared spectroscopy: Method and instrumentation optimisation. Postharvest Biol. Technol. https://doi.org/10.1016/j.postharvbio.2019.111078.
Sun, D., Cruz, J., Alcalà, M., Romero del Castillo, R., Sans, S., Casals, J., 2021. Near infrared spectroscopy determination of chemical and sensory properties in tomato. Journal of Near Infrared Spectroscopy. https://doi.org/10.1177/09670335211018759.
Szuvandzsiev, P., Helyes, L., Lugasi, A., Szántó, C., Baranowski, P., Pék, Z., 2014. Estimation of antioxidant components of tomato using VIS-NIR reflectance data by handheld portable spectrometer. International Agrophysics 28 (4).
Terada, M., Watanabe, Y., Kunitoma, M., Hayashi, E., 1979. Differential rapid analysis of ascorbic acid and ascorbic acid 2-sulfate by dinitrophenilhydrazine method. Ann. Biochem. Exp. Med. 4, 604–608.
Tilahun, S., Seo, M.H., Hwang, I.G., Kim, S.H., Choi, H.R., Jeong, C.S., 2018. Prediction of lycopene and β-carotene in tomatoes by portable chroma-meter and VIS/NIR

spectra. Postharvest biology and technology 136, 50–56. https://doi.org/10.1016/j.postharvbio.2017.10.007.

Tiwari, G., Slaughter, D.C., Cantwell, M., 2013. Nondestructive maturity determination in green tomatoes using a handheld visible and near infrared instrument. Postharvest Biology and Technology 86, 221–229. https://doi.org/10.1016/j.postharvbio.2013.07.009.

Torres, I., Pérez-Marín, D., De La Haba, M.J., Sánchez, M.T., 2015. Fast and accurate quality assessment of Raf tomatoes using NIRS technology. Postharvest Biol. Technol. https://doi.org/10.1016/j.postharvbio.2015.04.004.

Walsh, K.B., Mcglone, V.A., Han, D.H., 2020. The uses of near infra-red spectroscopy in postharvest decision support: a review. Postharvest Biol. Technol. 163, 111139 https://doi.org/10.1016/j.postharvbio.2020.111139.

Wang, F., Li, Y., Peng, Y., Wang, W., Zheng, X., 2016. Detection of Solid-acid Value of Tomato during Storage Using NIR Spectroscopy. In 2016 ASABE Annual International Meeting (p . 1). American Society of Agricultural and Biological Engineers. https://doi.org/10.13031/aim.20162460415.

Wati, R.K., Pahlawan, M.F.R., Masithoh, R.E., 2021. Development of calibration model for pH content of intact tomatoes using a low-cost Vis/NIR spectroscopy. In IOP Conference Series: Earth and Environmental Science, 686:(1), 012049; (2021, March) IOP Publishing.

Whitlow, T.H., Bassuk, N.L., Ranney, T.G., Reichert, D.L., 1992. An improved method for using electrolyte leakage to assess membrane competence in plant tissues. Plant Physiol. Minneapolis 98, 198–205.

Windig, W., Shaver, J., Bro, R., 2008. Loopy MSC: a simple way to improve multiplicative scatter correction. Appl. Spectrosc. https://doi.org/10.1366/00037020878604909.

Wu, G., Wang, C., 2014. Investigating the effects of simulated transport vibration on tomato tissue damage based on vis/NIR spectroscopy. Postharvest biology and technology 98, 41–47. https://doi.org/10.1016/j.postharvbio.2014.06.016.

H. Q. Yang , B. Y. Kuang , A. M. Mouazen , Size estimation of tomato fruits based on spectroscopic analysis. In Advanced Materials Research 2011; (Vol. 225, pp. 1254-1257). Trans Tech Publications Ltd. DOI: doi.org/10.4028/www.scientific.net/AMR.225-226.1254.

H. Yang , B. Kuang , A. M. Mouazen , In situ Determination of Growing Stages and Harvest Time of Tomato (Lycopersicon Esculentum) Fruits Using Fiber-Optic Visible—Near-Infrared (Vis-NIR) Spectroscopy. Applied Spectroscopy, 2011; 65(8), 931–938. https://doi.org/10.1366/11-06270.

Yang, H.Q., 2011. Nondestructive Prediction of Optimal Harvest Time of Cherry Tomatoes Using VIS-NIR Spectroscopy and PLSR Calibration. Advanced Engineering Forum 1, 92–96. https://doi.org/10.4028/www.scientific.net/aef.1.92.

Zhang, D., Yang, Y., Chen, G., Tian, X., Wang, Z., Fan, S., Xin, Z., 2021. Nondestructive evaluation of soluble solids content in tomato with different stage by using Vis/NIR technology and multivariate algorithms. Spectrochimica Acta Part A: Molecular and Biomolecular Spectroscopy 248, 119139. https://doi.org/10.1016/j.saa.2020.119139.

Zhu, Q., He, C., Lu, R., Mendoza, F., Cen, H., 2015. Ripeness evaluation of 'Sun Bright' tomato using optical absorption and scattering properties. Postharvest Biology and Technology 103, 27–34. https://doi.org/10.1016/j.postharvbio.2015.02.007.